Sachse, V., Anka, Z., Littke, R., Rodriguez, J. F., Horsfield, B., di Primio, R. (2016): Burial, temperature and maturation history of the austral and western Malvinas Basins, southern Argentina, based on 3D basin modelling. - *Journal of Petroleum Geology*, *39*, 2, pp. 169—191.

DOI: http://doi.org/10.1111/jpg.12639

BURIAL, TEMPERATURE AND MATURATION HISTORY OF THE AUSTRAL AND WESTERN MALVINAS BASINS, SOUTHERN ARGENTINA, BASED ON 3D BASIN MODELLING

V.F. Sachse[1,2 *], Z. Anka[1, 4], R. Littke2, J. F. Rodriguez[3], B. Horsfield[1] and R. di Primio[1, 5]

[1] GFZ German Research Centre for Geosciences, Helmholtz Centre Potsdam,Telegrafenberg; 14473 Potsdam, Germany.

[2] Energy and Minerals Resources (EMR), Institute of Geology and Geochemistry of Petroleum and Coal, RWTH Aachen University, Lochnerstr. 4-20, 52056 Aachen, Germany.

[3] Petrobras Argentina S.A., Buenos Aires, Argentina.

[4] present address: TOTAL Exploration - New Ventures, Paris, France.

[5] present address: Lundin Norway AS, PO Box 247, N-1326 Lysaker, Norway.

*Corresponding Author: victoria.sachse@emr.rwth-aachen.de

This paper presents a numerical petroleum systems model for the Jurassic-Tertiary Austral (Magallanes) Basin, southern Argentina, incorporating the western part of the nearby Malvinas Basin. The modelling is based on a recently published seismo-stratigraphic interpretation and resulting depth and thickness maps. Measured vitrinite reflectance data from 25 wells in the Austral and Malvinas Basins were used for thermal model calibration; eight calibration data sets are presented for the Austral Basin and four for the Malvinas Basin. Burial history reconstruction allowed eroded thicknesses to be estimated and palaeo heat-flow values to be determined. Six modelled burial, temperature and maturation histories are shown for well locations in the onshore Austral Basin and the western Malvinas Basin. These modelled histories, combined with kinetic data measured for a sample from the Lower Cretaceous Springhill Formation, were used to model hydrocarbon generation in the study area. Maps of thermal maturity and transformation ratio for the three main source rocks (the Springhill, Inoceramus and Lower Margas Verdes Formations) were compiled. The modelling results suggest that deepest burial occurred during the Miocene followed by a phase of uplift and erosion. However, an Eocene phase of deep burial leading to maximum temperatures cannot be excluded based on vitrinite reflectance and numerical modelling results. Relatively little post-Miocene uplift and erosion (approx. 50-100 m) occurred in the Malvinas Basin.

Based on the burial- and thermal histories, initial hydrocarbon generation is interpreted to have taken place in the Early Cretaceous in the Austral Basin and to have continued until the Miocene. A similar pattern is predicted for the western Malvinas Basin, with an early phase of hydrocarbon generation during the Late Cretaceous and a later phase during the Miocene. However, source rock maturity (as well as the transformation ratio) remained low in the Malvinas Basin, only just reaching the oil window. Higher maturities are modelled for the deeper parts of the Austral Basin, where greater subsidence and deeper burial occurred.

Key words: Basin modelling, petroleum system, hydrocarbon generation, maturity, erosion, Austral Basin, Malvinas Basin, Argentina, South America.

INTRODUCTION

The Austral (Magallanes) foreland basin covers an area of about 195,000 km² on- and offshore SE Argentina (Zambrano and Urien, 1970) in Tierra del Fuego and Patagonia Provinces (Fig. 1A). To the east, it is separated by a basement high (Rio Chico High) from the offshore Malvinas Basin (Figs 1A, B). The fills of both basins comprise rocks of Jurassic to Quaternary ages which rest unconformably on Palaeozoic

basement (Fig. 2). The evolution of the Austral and Malvinas Basins is closely associated with the various phases of the Andean orogeny. Proven hydrocarbon resources occur in the Austral Basin but have not yet been located in the Malvinas Basin. This study is based on thermal maturity data from wells in the Austral and Malvinas Basins which were used to calibrate numerical petroleum systems models. The models took account of the tectonic and volcanic evolution of the Austral–Malvinas Basin system. The results of numerical modelling will add to the understanding of petroleum generation in the basins, and also address uncertainties with respect to petroleum generation and accumulation; they provide an example of a large-scale petroleum systems evaluation in a mature foreland basin system.

Exploration History

Hydrocarbon exploration in Tierra del Fuego Province including the Austral Basin began in the early part of the 20th century. Thomas (1949) recorded the discovery of several gas seeps and one oil seep in the Austral Basin, encouraging future exploration efforts. At the present day, a total of 28 blocks covering the entire basin area are operated by different companies, with a particular focus on Tierra del Fuego (Rossello *et al*., 2008).

In Tierra del Fuego, more than 1000 wells have been drilled and proven reserves are about 12.5 Mm^3 of petroleum and 15,750 Mm^3 of gas (Rossello *et al*., 2008). On- and offshore exploration is continuing both for conventional petroleum and for unconventional targets such as tight sandstones (Marinelli, 1998), coal bed methane (Rio Turbio field) and igneous reservoirs (Ghiglione *et al*., 2009). In Chile, the Tranquilo field (Fig. 1B) produces gas from a siliciclastic reservoir of Tertiary age. Tertiary (Paleogene) gas reservoirs are also exploration targets in the nearby Glencross area in Argentina (Fig. 1B). Positive test results in wells in the fold-and-thrust belt have encouraged recent exploration in this area. Wells in the Paso Fuhr block (e.g. Paso Fuhr es-1; Fig. 1B) recorded indications of gas, and oil shows are present in well Morro Chico x1 in Glencross field. Important oil and gas fields are located in the Strait of Magallanes (Condor field) and in the offshore Austral Basin (Carina and Aries fields) (Fig.1B).

In the Malvinas Basin, in spite of a geological history which is similar to that of the Austral Basin, neither commercial oil nor gas accumulations have been found, although hydrocarbon shows have recently been reported (Baristeas *et al*., 2012).

Structure and Tectonic Evolution

The Austral Basin is bordered by the Deseado Massif to the north and NE which continues to the south as the Rio Chico High separating the Austral and Malvinas Basins (Fig. 1). To the south and west, the Austral Basin is bordered by the Fuegian and Patagonian Andes. The Fuegian Andes and further east the North Scotian Ridge limit the Malvinas Basin to the south (Tassone *et al*., 2008).

The present study is based on detailed seismic and 1D backstripping analyses (Sachse *et al*., 2015), the results of which indicate three major tectonic phases in the Austral Basin (see also Galeazzi, 1998; Diraison *et al*., 2000; Ghiglione, 2002; Franzese *et al*., 2003; Rossello *et al*., 2008). These stages began with Jurassic rifting and the development of the Late Jurassic – Early Cretaceous back-arc Austral/Rocas Verdes Basin. In the Austral Basin, Middle to Late Jurassic sediments are represented by the Tobifera Formation (Fig. 2), which consists mainly of acid volcanic rocks and volcaniclastics (Pittion and Arbe, 1999). These are overlain unconformably by sandstones and shales (Continental Springhill at the base) and marine shales (Marine Springhill above) of the Springhill Formation, then Barremian to Early Aptian marine shales and siltstones of the Lower Inoceramus Formation (Pampa Rincon Formation*). This formation reaches a maximum thickness in the SW of the Austral Basin and onlaps the Rio Chico High. The source of sediments in the Early Cretaceous was from the north and east. Above are marine marls of the mid-Aptian Margas Verdes Formation (Nueva Argentina Formation*), shales of the mid Cenomanian to mid Coniacian Middle Inoceramus Formation (Arroyo Alfa Formation*), and shales of the Upper Inoceramus Formation (Cabeza de Leon Formation*) which is mid-Coniacian to Maastrichtian in age.

(*The stratigraphy is described here using the most commonly-used formation names; in brackets are local formation names which are used for Tierra del Fuego (Fig. 2; Robbiano et al., 1996).)

An inversion phase occurred in the early Late Cretaceous, and subsequent evolution of the Austral Basin was associated with the development of the Patagonian Andes fold-and-thrust belt during the Paleocene and Eocene. Thermal and flexural subsidence occurred (Sachse *et al*., 2015) beginning at approximately 90 Ma, with the depocenter progressively migrating eastwards. Uplift and erosion of the Andes since the Late Cretaceous provided a new sediment source to the south, west and NW of the basin. Sediments were initially deposited in a deepmarine setting, but depositional conditions gradually shallowed over time and Eocene and later sediments are continental.

Seismic interpretations of the Upper Cretaceous to Lower Tertiary sedimentary succession in the Austral Basin show thickening towards the west and SW (Sachse *et al*., 2015), towards the fold-and-thrust belt (Suarez *et al*., 2000). Subsidence is interpreted to be due to lithospheric loading and flexure starting in Maastrichtian to Paleocene times, and the asymmetric basin structure is typical of that of a foreland basin (Allen and Allen, 2013) (Fig. 3). The Upper Cretaceous to Lower Tertiary succession is up to 5000 m thick (Biddle *et al*., 1986; Sachse *et al*., 2015) (Fig. 3). Phases of uplift during the Paleogene and Neogene were associated with volcanic activity (Figs. 2) and the emplacement of sills, dykes and intrusions (Kay *et al*., 2004).

The geological history of the Malvinas Basin is broadly similar to that of the Austral Basin, although opening of the South Atlantic had a major impact on the development of the former basin. During the Cretaceous, thermal cooling led to basin subsidence (Ghiglione *et al*., 2010), whereas a compressional regime occurred since the Late Cretaceous in the Austral Basin due to the development of the Andean orogen. During the Paleocene and Early Eocene, the opening of the Drake Passage affected the Malvinas Basin (Ghiglione *et al*., 2010) due to changes in major stress directions, and a compressional foreland setting developed since the Late Eocene passing into a transpressional setting during the Oligocene (Tassone *et al*., 2008; Ghiglione *et al*., 2010). From the latest Miocene onwards, the Malvinas Basin mostly received sedimentary material transported through the overfilled Austral Basin, and in addition received sediments derived from the Fuegian Andes (Fig. 1) (Baristeas *et al*., 2013, Sachse *et al*., 2015).

Stratigraphy and Petroleum System Elements

Geochemical studies have been carried out on samples from the Austral Basin and adjacent areas (i.e. Pittion and Gouadain, 1992; Pittion and Arbe, 1999; Biddle *et al*., 1986; Galeazzi *et al*., 1998; Rossello *et al*., 2008). These investigations indicated that organic-rich Lower Cretaceous intervals had good source rock potential while Upper Cretaceous and Tertiary units may act as potential reservoir rocks (Fig. 2). The main reservoir is the Lower Cretaceous Springhill Formation.

The Upper Jurassic Tobifera Formation (Fig. 2) in general consists of rhyolites and basalts, volcanic breccias and tuffs, together with conglomerates, sandstones and shales deposited in continental to lacustrine settings (Biddle *et al*., 1986). Organic-matter rich shale intervals may have source rock potential (Galeazzi, 1998; Cagnolatti *et al*., 1996) although they are only locally developed. The Estancia Dos Lagunas field in Santa Cruz Province produces gas mainly from volcanic reservoir rocks in the Tobifera Formation (Hinterwimmer, 2002; Sruoga and Rubinstein, 2002, 2007; Sruoga *et al*., 2004).

The unconformably overlying fluvial sandstones, shales and coaly intervals of the Lower Cretaceous continental Springhill Formation contain Type II/III kerogen (TOC 2-6%); above are shales and sandstones of the marine Springhill Formation up to 200 m thick. Both formations are source rocks in the Austral Basin, while the continental Springhill Formation also has reservoir potential (e.g. Pittion and Gouadain, 1992; Pittion and Arbe, 1999; Biddle *et al*., 1986; Galeazzi *et al*., 1998; Rodriguez *et al*., 2008; Rossello *et al*., 2008). Organic matter in the marine Springhill Formation is of mixed marine and terrestrial origin with

a low petroleum generation potential, as shown by TOC contents of 0.4 to 0.9 % and low HI values (80-300 mg/g TOC).

Barremian to Early Aptian marine shales and siltstones of the Lower Inoceramus Formation, 50 to 150 m thick, contain black shales with Type II kerogen, and are overlain by marls of the mid-Aptian Margas Verdes (Nueva Argentina) Formation. Although TOC values in the Lower Inoceramus Formation are low (0.6 to 1.3 %), the quality of organic matter is good (HI 300-700 mg/g TOC). In the Margas Verdes Formation, organic matter is enriched in a 30- 40 m thick interval in the lower part of the unit in which mixed planktonic and terrestrial organic matter occurs (Types II and II/ III kerogen), with TOC varying between 1.5 and 2 % (Rodriguez *et al*., 2008).

The Lower Inoceramus and Margas Verdes Formations are overlain by shales of the mid- Cenomanian to mid-Coniacian Middle Inoceramus (Arroyo Alfa) Formation, and the deep-marine to deltaic shales of the Upper Inoceramus (Cabeza de Leon) Formation of mid-Coniacian to Maastrichtian age (Natland *et al*., 1974). These sediments are associated with a first northward transgression of the proto South Atlantic/Weddell Sea over Patagonia and western Argentina (Wilson, 1991; Pittion and Arbe, 1999). During the Late Cretaceous, the Austral Basin became more continental in the west and only a minor area in the east remained marine (Wilson, 1991). Since the late Early Paleocene, alluvial and lacustrine settings covered the central and northern parts of Patagonia, while the southern tip remained marine (Ortiz-Jaureguizar and Cladera, 2006). Deposition during the Paleocene to Oligocene was dominated by sandstones together with shales, conglomerates and marls. The occurrence of glauconite in the Lower Magallanes Formation (Maastrichtian to Eocene) suggests shallow-marine depositional conditions. The Upper Magallanes Formation (Oligocene to Early Miocene) consists of silts and shales deposited in a fluvial to shallow-marine setting. Miocene sediments were mainly deposited in continental to shallow-marine conditions and comprise the Santa Cruz (fluvial to alluvial) and Patagonia Formations.

The main reservoir units in the Austral Basin are the Upper Jurassic – Lower Cretaceous sandstones of the Springhill Formation, which were deposited in a fluvial-deltaic to shallow-marine environment. To the west, slope channels and basin floor turbidites are potential reservoir units, and more minor reservoirs include Maastrichtian – Eocene glauconitic sandstones and carbonates (Galeazzi *et al*., 1998; Rossello *et al*., 2008).

The formation of structural traps was related to the reactivation of rift-related Triassic – Late Jurassic faults, and to folds and faults in the Springhill Formation. Mudstones in the Springhill, Inoceramus, Margas Verdes and Lower Magallanes Formations may act as seals (Fig. 2).

METHODS

Vitrinite Reflectance

Thermal calibration data in terms of vitrinite reflectance values and measured temperature data were provided by Petrobras S.A., and wells used for calibration purposes are shown in Fig. 4. For calculations of vitrinite reflectance as a calibration parameter for heat flow during maximum burial (Senglaub *et al*., 2006), the Easy%Ro algorithm (Sweeney and Burnham, 1990) was used. The algorithm is applicable for a VR_r range between 0.3% and 4.6%.

Kinetics of petroleum generation

The kinetics of petroleum formation were determined for an organic-rich sample from the Lower Cretaceous Springhill Formation, chosen on the basis of its high total organic carbon content of 68.6 %. The sample was recovered from an outcrop in eastern Patagonia. The sample was analyzed by non-isothermal open system pyrolysis at four different heating rates (0.7, 2.0, 5.0 and 15 °C/min) using a Source Rock Analyzer© (Humble Instruments and Services, Inc.). The pyrolysis products were transported to a FID in a constant He flow (50 mL/ min). Low heating rates were used to avoid heat transfer problems

which may influence the product evolution curves, and consequently the geological predictions (Schenk and Dieckmann, 2004). The generated bulk petroleum formation curves served as input for a bulk kinetic model consisting of an activation energy distribution and a single pre-exponential factor. The discrete activation energy distribution with a single frequency factor was determined using Kinetics 2000 software (Burnham *et al*., 1987).

Input data

Basin and petroleum systems modelling follows the principles described by Welte and Yükler (1981), Welte and Yalcin (1988), Poelchau *et al*. (1997), Welte *et al*. (1997) and Hantschel and Kauerauf (2009). A finite-element forward model was created to simulate the burial history of sediments in the Austral Basin and Malvinas Basin taking into account compaction, pressure, temperature and maturation of organic matter, and petroleum generation through time. The model was constructed using PetroMod 2012.1 software (Schlumberger, Germany). Input data include present-day basin architecture derived from 2D seismic profiles (Sachse *et al*., 2015). Fourteen stratigraphic intervals were included in the 3D basin model which extended between the Jurassic Tobifera Formation and the present-day topographic/sea-level surface. The modelled area (Figs 1, 3) was 654 km long from west to east and 345 km from north to south, and was calculated with a cell size in the horizontal plane of 2 x 2 km. The area includes the onshore and offshore Austral Basin, the Rio Chico High and the western Malvinas Basin.

Stratigraphy and thickness variations

The stratigraphic thickness values for the Mesozoic and Cenozoic successions are based on seismic stratigraphic analyses (Sachse *et al*., 2015). The stratigraphic units used in the modelling are based on Biddle *et al*. (1986), Pittion and Gouadain (1992), Galeazzi (1998), Olivero and Martinioni (2001), Franzese *et al*. (2003) and Olivero and Malumián (2008), and chronostratigraphy is based on Robbiano *et al*. (1996).

For the model, the following stratigraphic units were recognized: Tobifera Formation; Lower Inoceramus (Pampa Rincon Formation) and Margas Verdes Formation (not divided); Middle (Arroyo Alfa Formation) and Upper Inoceramus (Cabeza de Leon) Formations; Upper Palermo Aike Formation; Paleocene, Eocene, Oligocene (Lower Magallanes); Santa Cruz and Patagonia (not divided); and Plio- Pleistocene (Figs 2, 5). To assign the potential source rock layers of Early Cretaceous age in the model, the interval was split into five uniform layers representing the Upper Margas Verdes Formation, the Lower Margas Verdes Formation, the Inoceramus Formation, the marine Springhill Formation and the continental Springhill Formation. This simple layer-splitting approach may result in slight under- or over-estimation of layer thicknesses, but could not be avoided due to the limited data on the exact thicknesses of the specific source rock intervals in the study area.

In general, the Mesozoic-Cenozoic stratigraphy is thickest in the SW Austral Basin, thins to the east above the Rio Chico High, and thickens to the SE in the Malvinas Basin (Fig. 3). At the base of the stratigraphic column is the Jurassic Tobifera Formation (Fig. 2), the thickness of which varies between up to 1200 m in the central and southern Austral Basin, and up to 1600 m in the western Malvinas Basin. Over the Rio Chico High, it is up to 250 m thick. Overlying Lower Cretaceous sediments have a maximum thickness of 3000 m in the SW Austral Basin, and are 1000 m thick in the central part. A thickness of about 1000 m is observed for the southeastern most part of the study area in the Malvinas Basin (Fig. 3).

The total thickness of Upper Cretaceous sediments is up to 4500 m in the southern Austral Basin, thinning to 2500 m towards the NW. On the Rio Chico High the unit is on average 500 m thick.

In the NW Austral Basin and SE Malvinas Basin, the Paleocene interval is up to 1400 m thick, but is only about 100 m thick over most of the Austral Basin, the Rio Chico High and the western Malvinas Basin. The Eocene is up to 1000 m thick in the SW and central Austral Basin and SE Malvinas Basin. Oligocene

sediments reach a thickness of up to 1000 m in the western part of the Austral basin, thinning to 150 m in the NE and less than 50 m in the NW, SW and south. Thickness information for the Malvinas Basin was not available as no identification of the Oligocene layer was possible due to missing well pick information, and thus the Oligocene was assigned as part of the Miocene.

The Miocene reaches maximum thicknesses of 800 m in the SW and central Austral Basin, thinning to 200 m in the north and east; lower values are found on the Rio Chico High with a minimum of 30 m. In the western Malvinas Basin, the Miocene is up to 3000 m in thickness in the south, decreasing to the north, NW and NE to minimum values of less than 50 m.

Erosional phases

Three erosional events (corresponding to unconformities) are suggested to have occurred in the Austral Basin (Biddle *et al*., 1986; Galeazzi, 1998) (Fig. 2): Jurassic erosion at about 150 Ma, with a maximum eroded thickness of 75 m; Maastrichtian erosion (at about 68 Ma), with a maximum eroded thickness of 250 m; and an Eocene erosional phase with a maximum eroded thickness of 250 m at about 42.5 Ma. The Jurassic erosional event was not integrated into the model because it did not affect the burial history with respect to potential source rock deposition and maturation. For modelling, the present-day thickness of the Late Cretaceous and Eocene was subtracted from the assumed initial thickness, bearing in mind values from previous publications (Biddle *et al*., 1986; Galeazzi, 1998). The erosion events, their localities and their durations are of course simplifications, but this will have little effect on the modelling results except in the Paso Fuhr area due to the great thicknesses there of eroded sediments *(see below*). Maps of eroded thickness are presented in Fig. 6.

Upper and Lower Boundary conditions

Igneous intrusive bodies at different levels in the stratigraphic column have been recorded in the Austral Basin (Ghiglione *et al*., 2009; Hubbard *et al*., 2007; Kay *et al*., 2004; Sachse *et al*., 2015) (Fig. 5). Uyeda *et al*., (1978) and Zielinski and Bruchhausen (1983) reported heat flow anomalies in Tierra del Fuego, and the geothermal gradient was calculated to be 32 °C/km (Uyeda *et al*., 1978) or 34.6±2.5 °C/km (Zielinski and Bruchhausen, 1983). These values were interpreted by these authors to be due to the presence of circulating hydrothermal fluids. A single heat flow value of 96 mW/m² was published by Uyeda *et al*., (1978) based on the geothermal gradient of 32°C/km. The nearby subduction zones to the west (Antarctic Plate), as well as the transform boundary between the South American and Scotian Plates, may have been responsible for the circulation of hydrothermal fluids in the study area, together with volcanic activity and increased heat flows, and were tested in the model (*see below*).

Palaeo bathymetric maps of the study area were constructed following Natland *et al*. (1974), Wilson (1991) and Pittion and Arbe (1999). Variations in the extent of the deep-water regions were assumed over time, as deep-water conditions prograded to the east (Sachse *et al*., 2015). Thus during the Jurassic, an elongated palaeo deep-water zone (maximum depth 500 m) occurred parallel to the present-day Andes, expanding during the Early and Middle Cretaceous to the NE. During the Late Cretaceous (max. 250 m depth) and Paleogene, deep-water zones were located in the central and eastern parts of the Austral Basin (Wilson, 1991). At the present day, the deepest waters are located in the eastern part of the western Malvinas Basin (280 m). Detailed palaeo water-depth maps were published by Sachse *et al*. (2015). Based on the palaeo water depth, the sediment-water interface temperature (SWIT) was calculated for latitude 56° in South America (Wygrala, 1989).

RESULTS

Erosion

For modelling, the present-day thicknesses of the Late Cretaceous and Eocene intervals were subtracted from the assumed initial thicknesses, resulting in palaeo-thickness values (maps of eroded thickness are

presented in Fig. 6). The Cretaceous erosion event began in the Maastrichtian (68 Ma) and had a duration of 2.5 Ma (Ghiglione *et al*., 2009). Erosion was probably associated with a compressional phase and uplift of the northern and western areas and Rio Chico High (Ghiglione *et al*., 2009). The Eocene erosion event was set to a duration of 5 Ma, starting at 42.5 Ma, and is related to a strike-slip phase coupled with compression (Ghiglione *et al*., 2010). It should be noted that this erosional phase is highly speculative in time and space.

Uplift of the Patagonian Andes occurred since the Miocene and was related to the Quechua orogenic phase (Ortiz-Jaureguizar and Cladera, 2006). A late Miocene to Recent erosional event was therefore assigned to the model. This event mainly affected the NW part of the study area and led to erosion of up to 800-1000 m of sediments in the Paso Fuhr region, with thicknesses decreasing to the SE (Biddle *et al*., 1986; this study). The duration of this event was set to 10 Ma. The eastern Austral Basin, the Rio Chico High and the Malvinas Basin were not affected.

Regional extension and the duration and intensity of erosional events were taken into account with generalized values, but this had little effect on the modelling results except in the Paso Fuhr area due to the thicknesses of sediments eroded.

The most recent erosion events did not affect the Malvinas Basin, as the sedimentary filling and the erosional history of the basins is different. In particular, major sediment supply has occurred in the Malvinas Basin since the Miocene, and as a consequence only minor thicknesses have been eroded since then.

Heat Flow

For the reconstruction of the thermal history and the evaluation of source rock maturity and petroleum generation, the palaeo heat flow history was determined. It should be noted that heat flow was only calibrated for times of maximum burial and for the present day. Heat flow maps for different time steps are presented in Fig. 7. Present-day heat flow is around 65 to 70 mW/ m² in most parts of the Austral Basin, declining on the Rio Chico High to 58 mW/m² and about 50 mW/ m² in the Malvinas Basin, increasing to the SE most margin (Fig. 7).

Elevated palaeo heat flows were assigned for the Jurassic rift phase, with maximum values of 80 mW/ m². Episodes of volcanic activity during the Paleogene, Neogene and at the present day were incorporated, with maximum heat flows of 85 mW/m². Although temperature increases in the vicinity of dykes and sills due to igneous intrusions and hydrothermal fluids was local and short-lived, it may have influenced source rock maturation. A general heat flow trend is assigned in Fig. 8B.

Burial, thermal and maturation history

The maturity history in terms of burial and thermal evolution was calibrated using measured and calculated vitrinite reflectance data reflecting maximum temperatures during burial. This data was provided by Petrobras Argentina for eight exploration wells in the onshore Austral Basin and four wells in the Malvinas Basin. The calibration data is shown in Fig. 4. The burial history for four wells in the Austral Basin (wells 1-4: Figs 1B, 4) and two wells in the Malvinas Basin (wells 10, 12; Figs 1B, 4) is discussed in detail in the following paragraphs. The wells were created using the extraction tool in 3D and for comparison also created in 1D. Organic-matter maturation and transformation is evaluated for three potential source rock intervals: the Early Cretaceous Springhill Formation; the Early Cretaceous Inoceramus Formation; and the Early Cretaceous Lower Margas Verdes Formation.

(i) Well 1, northern Austral Basin

The 1D burial history for Well 1 in the northern part of the Austral Basin (Fig. 8A; location in Fig. 4) shows that potential source rocks in the Lower Cretaceous Springhill Formation were buried to shallow

depths until approximately 83 Ma (mid-Late Cretaceous). As a result of increased sediment supply from the eroding Andes, the Springhill Formation was then buried to a depth of about 900 m (at 68 Ma), followed by Maastrichtian uplift and erosion of about 100 m of section. Palaeo temperatures reached 45 °C, and vitrinite reflectance 0.32 %R_r. Smooth uplift then followed until the end of the Eocene.

During the Oligocene and early Miocene, Springhill Formation sediments were buried again, finally reaching maximum burial depths of 1350 m. A palaeo temperature maximum (72°C) was reached at about 5 Ma, corresponding to VR_r values of 0.44 % (Fig. 8B). As the potential source rock units are very thin in the northern Austral Basin, minor palaeo temperature variations (differences of 1-3°C) and corresponding maturity values occur for the overlying Inoceramus and Lower Margas Verdes Formations.

(ii) Well 2, central Austral Basin

Well 2 in the central Austral Basin (Fig. 4) shows much deeper burial of the Lower Cretaceous Springhill Formation until the Maastrichtian erosional event, when some 120 m of section was removed (Fig. 9A). At 67 Ma, the Springhill Formation had reached a depth of 2200 m and a corresponding temperature of 130 °C. The Inoceramus and Lower Margas Verdes Formations show temperatures of 122°C and 116°C, respectively. VR_r values are 0.84% for the Springhill Formation, 0.79% for the Inoceramus Formation and 0.75% for the Lower Margas Verdes Formation (Fig. 9B), resulting in significant differences in transformation ratios.

Following Maastrichtian uplift and erosion and a short-lived burial phase until the end of the Paleocene, the sediments were uplifted again culminating in the Eocene erosion event when about 100 m of section was removed (Fig. 9A). Deep burial occurred at the beginning of the Oligocene, finally resulting in maximum burial for the Springhill Formation of about 3000 m. The highest palaeo temperatures of 143°C were reached at about 5 Ma, corresponding to VR_r values of about 1.07 % for the Springhill Formation, 1.0 % for the Inoceramus Formation (139°C) and 0.96 % for the Lower Margas Verdes Formation (136°C) (Fig. 9B). Erosion since 5 Ma has resulted in the present-day depth of the Springhill Formation of 2668 m at this well location.

(iii) Well 3, southern Austral Basin

At well 3 (Fig. 4), there was progressive burial of the Springhill Formation until about 83 Ma followed by a rapid increase in the burial rate, resulting in a depth of 5600 m for the formation at 68 Ma (Fig. 10A), 5200 m for the Inoceramus Formation, and 4860 m for the Lower Margas Verdes Formation. Palaeo temperatures reached 281°C for the Springhill Formation, 252°C for the Inoceramus Formation and 231°C for the Lower Margas Verdes Formation, and corresponding VR_r values for the three formations are 3.95 %, 3.38 % and 2.92 % (Fig. 10 B).

Burial during the next 63 Ma reached a maximum at 6 Ma, with a depth of 7050 m for the Springhill Formation, 6700 m for the Inoceramus Formation and 6400 m for the Lower Margas Verdes Formation. Maximum palaeo temperatures for the three formations are 343°C, 322°C and 304°C with corresponding VR_r values of >4.6 % (Springhill and Inoceramus Formations, Fig. 10B) and 4.6 % (Lower Margas Verdes Formation). Subsequent uplift resulted in present-day depths at this well location of 6778 m for the Springhill Formation, 6387 m for the Inoceramus Formation, and 5668 m for the Lower Margas Verdes Formation.

(iv) Well 4, western Austral Basin

Well 4 in the western Austral Basin (Fig. 4) shows a generally similar burial history to that observed at well 3 in the southern part of the basin (Fig. 11). Following burial of the Springhill Formation to depths of about 1800 m (108°C/0.67%VR_r) at 68 Ma (Fig. 11A), Maastrichtian erosion occurred but was immediately followed by burial until the Eocene erosion event. A subsequent phase of burial resulted in maximum burial depths (3500 m for the Springhill Formation) and the highest palaeo temperatures and maturities

(214°C/2.6 %VR_r; Fig. 11B). Intense erosion has taken place since the Miocene (5 Ma) resulting in the present-day depth of the Springhill Formation of 2600 m at well 4 (Fig. 11A). The Inoceramus Formation shows palaeo temperatures of 200°C and VR_r of 2.3 % for the time of maximum burial (Fig. 11B); the Lower Margas Verdes Formation shows values of 190°C at 2 %VR_r (Fig. 11B).

(v) Well 10, central Malvinas basin

The Springhill Formation at Well 10 in the central Malvinas Basin (Fig. 4) reached a depth of 971 m at the end of the Late Cretaceous, corresponding to a temperature of 36°C (0.30 %VR_r) (Fig. 12A). After a smooth uplift phase, further burial occurred during the Paleocene and Eocene, followed by a short phase of uplift and non-deposition. Further deepening of the basin was initiated since the end of the Oligocene. The present-day depth of the Springhill Formation is 1270 m (39°C/0.33 %VR_r; Fig. 12B). Highest temperatures were reached in the late Paleocene (43°C/0.32%VR_r). The Inoceramus Formation shows maximum palaeo temperatures of 40°C and VR_r of 0.31 % for the end of the Paleocene; the Lower Margas Verdes Formation shows values of 38°C at 0.30 %VR_r (Fig. 12B). Present-day temperatures are 36°C (0.33%VR_r) for the Inoceramus Formation and 35°C (0.32%VR_r) for the Lower Margas Verdes Formation (Fig. 12B).

(vi) Well 12, eastern Malvinas basin

Well 12 is located in the eastern Malvinas Basin (Fig. 4). At the end of the Late Cretaceous, the Springhill Formation reached a burial depth of 1608 m here (62°C/ 0.53%VR_r), followed by a smooth phase of uplift and deeper burial until the late Eocene (2026 m) (Fig. 13A). Erosion occurred in the late Eocene, but deposition of Miocene sediments led to further deepening. The present-day depth below sea level of the Springhill Formation is 2652 m. Highest palaeo temperatures occurred at the end of the Late Cretaceous (92°C), with a second maximum of 90°C at the end of the Miocene. Maximum maturities of 0.58 %VR_r since the late Miocene correspond to this temperature history. Present-day temperature is 79°C for the Springhill Formation (Fig. 13B). The Inoceramus Formation shows maximum palaeo temperatures of 84°C and VR_r of 0.5 % for the end of the Late Cretaceous; the Lower Margas Verdes Formation shows values of 79°C at 0.46 %VR_r (Fig. 13B). Present-day temperatures are 77°C (0.52 %VR_r) for the Inoceramus Formation and 73°C (0.5%VR_r) for the Lower Margas Verdes Formation (Fig. 13B).

Bulk kinetics

In accordance with published maturity information (i.e. Pittion, 1991), the organic matter of the investigated sample of the Lower Cretaceous Springhill Formation was classified as immature containing Type II/III kerogen. This is supported by Rock Eval pyrolysis data (HI: 250 mg HC/g TOC; OI: 30 mg CO_2/g TOC; T_{max} 430°C).

Pyrolysis product generation curves were used to calculate the kinetic parameters, which comprise a discrete activation energy distribution for first-order reactions with Arrhenius-type temperature dependence using a single pre-exponential (frequency) factor. The activation energy is characterized by a fairly narrow distribution, typical of Types II to II/III kerogen, and indicating a relatively homogeneous OM (Burnham *et al*., 1987; Espitalié *et al*., 1988; Reynolds and Burnham, 1995; Dessort *et al*., 1997). As the sample contains a high proportion of coaly particles, the TOC values may be overestimated compared to average values for the Springhill Formation.

The main activation energies of the Springhill sample ranges between 53 and 58 kcal/ mol with a frequency factor of 3.24E+14/sec (Fig. 14A). Using these bulk kinetic parameters, the generation rates and transformation ratios (temperature and timing of petroleum generation) were calculated for a heating rate of 3°C/Ma. This heating rate corresponds to an average value for sedimentary basins (Schenk and Dieckmann, 2004) and is also justified for the Austral-Malvinas Basin. Accordingly, petroleum generation is expected to take place in a temperature interval between 100 and 200°C, with peak generation at 140°C (Fig. 14B).

Timing of petroleum generation

Timing of petroleum generation is based on temperature and burial history and was calculated for potential source rock intervals in the Springhill Formation, using the Type II oil-gas kinetics of Pepper and Corvi (1995) for the Inoceramus and Lower Margas Verdes Formation and the previously described kinetic for the Springhill Formation. An obvious limitation is that the only sample analyzed may not be representative of the rest of the basin stratigraphy, in which lateral changes and variations in TOC (and even kerogen type) can be expected. However, Rock-Eval analysis of other organic-rich Springhill Formation samples from the same outcrop indicate only minor facies variability, and in the absence of samples from additional sites, it is acceptable to use the kinetics of this single sample instead of default kinetics. Furthermore, comparison of the present kinetic data set with the standard petroleum generation kinetics of Pepper and Corvi (1995) pointed to only minor differences, namely a slightly earlier onset of petroleum generation according to the Pepper and Corvi (1995) kinetics.

The model shows that no petroleum generation occurred at well 1 in the northern part of the Austral Basin (Fig. 8 B) before the Miocene, resulting in transformation ratios of only 1.3 % for the Springhill Formation and 1.2 % for the Inoceramus Formation (Fig. 9B). Although there are uncertainties in the model, these values suggest that no significant petroleum generation occurred. The Lower Margas Verdes Formation also did not generate petroleum in significant volumes, and the limited petroleum generation is not sufficient for petroleum expulsion to have occurred (Cooles *et al*., 1986; Rullkötter *et al*., 1987)

At well 2 in the central Austral Basin (Fig. 9), petroleum generation began at 97 Ma. The Springhill Formation reached a transformation ratio of 84 % at the end of the Late Cretaceous, the ratio remaining constant during the Paleogene and then increasing during the Miocene to a maximum of 96 % (Fig. 9B). The Inoceramus Formation shows lower ratio values of 76 % at 67 Ma, constant values through the Paleogene, which finally increase to 95 % (Fig. 9B). The Lower Margas Verdes Formation reached a transformation ratio of 42 % at 67 Ma; the ratio was unchanged during the Paleogene and then increased to 75 % at the end of the Miocene (Fig. 9B).

In the southern basin area (Well 3, Fig. 10), petroleum generation began in the Early Cretaceous, and the transformation ratio increased by the end of the Early Cretaceous to 76 % for the Springhill Formation and 12% for the Inoceramus Formation (Fig. 10B). Since 70 Ma, the transformation ratio reached 100 % for both the Springhill and the Inoceramus Formations. The Lower Margas Verdes Formation did not generate hydrocarbons at this location because its lithology was assigned as a sandstone following an internal well report.

At well 4 in the Paso Fuhr area in the western Austral Basin (Fig. 11), petroleum generation in the Springhill, Inoceramus and Lower Margas Verdes Formations began at the end of the Late Cretaceous. The Lower Margas Verdes Formation shows the strongest and most rapid increase in transformation ratio, reaching 55 % at 56 Ma (Fig. 11B). The Inoceramus and Springhill Formations show a smoother increase during the Late Cretaceous, reaching values of 11 % and 35 % at 67 Ma (Fig. 11B), respectively. Generation increased significantly during the Late Cretaceous / Paleocene. The highest transformation ratios were reached in the Paleocene, with values of 100 % for the Springhill and the Inoceramus and 97 % for the Lower Margas Verdes Formations (Fig. 11B).

The modelling suggests that highest palaeo temperatures and maturity ranges show a similar pattern for the three source rock intervals in the Austral Basin; therefore only the maps for the Springhill Formation are presented (Fig. 15A, B). The transformation ratio maps (Fig. 16) show the distribution of petroleum generation in the study area: the highest values for the Springhill (Fig. 16A) and Inoceramus (Fig. 16B) Formations occur in the deeper parts of the basin, and for the overlying Margas Verdes Formation in the southern and NW areas (Fig. 16C). Highest palaeo temperatures and maturities occurred in the southern and western parts of the basin, with vitrinite reflectance of up to 4.6 % (the maximum calculated by the EasyRo algorithm), indicating an overmature range (Fig. 15B). VR_r values of 4 % mark the limit of

commercial dry gas accumulations according to Dow (1977), and were reached since the Late Cretaceous. Maturity increased further in the Miocene (Fig. 11). This high maturity zone in the south is surrounded by areas of lower VR_r values which are in the gas window or overmature, with values up to 4.6 %VR_r (Figs 10B, 15B). Here, the highest maturities were reached since the Miocene. This is also true for the Paso Fuhr area (Fig. 15B), which reached gas window maturity during the Miocene (Figs 11B, 15B).

The oil window corresponds to VR_r values ranging between 0.55 and 1.3 %. At well 2 in the central part of the Austral Basin (Fig. 9), source rocks are in the oil window and the highest maturities were reached from the Miocene to the present day. The northern part of the study area and the offshore areas are immature with respect to petroleum generation (Figs 15, 16). The source rock transformation ratio is not modelled to exceed 1.2 % (Springhill Formation; Fig. 16A), although maturity increased during the Miocene (Fig. 8).

The modelling calculations for the Malvinas Basin show that the beginning of petroleum generation occurred in the Late Cretaceous. However, the transformation ratio remained low in the central part of the basin but increases to the east (well 12, Fig. 13). Since the Late Cretaceous, the transformation ratio continuously increased in the central basin, reaching its highest value at the present day (0.05 %). Higher values are calculated for well 12 (Fig. 13 B), where the Cretaceous source rocks are buried to greater depths. Transformation increased through time, but a first peak of the transformation ratio was reached at the end of the Late Cretaceous and a second peak at the end of the Miocene, resulting in transformation ratios of 4 % at the present day. Calculated transformation ratios for the Inoceramus and Lower Margas Verdes Formation show a similar pattern to that of the Springhill Formation, but with slightly lower values. As uncertainties cannot be excluded for such models, the petroleum generation for the Malvinas Basin can be regarded as zero.

Sensitivity Analyses

A series of sensitivity analyses in terms of different heat flow and erosion scenarios was carried out for well 4 in the Paso Fuhr area in the western Austral Basin. This is the only area where the calibration seems to depend to a great extent on heat flow and erosion, especially since the late Miocene. Considering measured vitrinite reflectance values of 1.8 % for the Lower Margas Verdes Formation, a “maximum heat flow” scenario was created, with a heat flow of 120 mW/m² since the late Miocene and no Miocene to present-day erosion (Scenario 1). This resulted in a fairly good match with measured vitrinite reflectance data for the Paleocene and Upper Cretaceous intervals. Nevertheless, the calculated vitrinite reflectance was too low when compared to measured values in the Oligocene and Miocene, and too high for the measured values in the Campanian and the layers below (Fig. 17). Despite the fact that magmatism occurred in this area resulting in elevated heat flow values, the assigned heat flow seems to be too high.

A second modelling scenario was created (Scenario 2), in which the final phase of Miocene/ post- Miocene uplift led to an erosion of 1800 m. The heat flow was set to 75 mW/m² since the late Miocene. In this scenario, a good calibration match was achieved with all the measured vitrinite reflectance values, but the erosion values seemed to be too high considering the regional geology and stratigraphy.

Therefore a third scenario was created (Scenario 3), with a late Miocene to present-day uplift event leading to 900 m of erosion and a heat flow of 75 mW/m². This scenario resulted in under-estimation of the measured vitrinite reflectance values (Fig. 17).

Because of the unknown erosion values, and to avoid over-estimation of both the palaeo heat flows and the erosional thicknesses, a scenario with a heat flow of 95 mW/m² and erosion of 800 m since the late Miocene was preferred, as described in the Results (*above*). This scenario best matches the calibration data and is also consistent with the geological evolution and with measured Eocene coal samples from the Rio Turbio Formation in the Santa Cruz Province (0.5- 0.58%VR_r; Villar *et al*., 1988)

Thermo-chronological measurements on outcrop samples from the western Magallanes Basin (Fosdick *et al.*, 2014) indicated maximum burial between 54 and 46 Ma, corresponding to palaeo temperatures for the Maastrichtian Dorotea Formation of 164-180 °C. Based on this information, a "Scenario 4" was created, assuming 800 m of erosion since the late Miocene and a total erosion of 2000 m for the Eocene. The heat flow values were set to 75 mW/m² since the Miocene, and to 100 mW/m² during the Eocene as magmatism occurred. The calibration curve for the vitrinite reflectance values (Fig. 17) shows a good match between measured and calculated values for the Paleocene interval and below, but a match with values above was not achieved. Furthermore, despite the high heat flow values and the high value for the Eocene erosion, the top-Cretaceous interval only achieved a palaeo temperature of about 143°C for the mid-Eocene according to this scenario, which is lower than predicted from thermochronology data (*see above*).

These sensitivity analyses imply that at least two evolutionary scenarios are possible to explain the burial history of the Austral Basin, with deepest burial occurring either during the Eocene or during the Miocene. The "Miocene scenario" is preferred here, as moderate values for the amount of erosion and for palaeo heat flow were sufficient to achieve a good calibration match with the measured vitrinite reflectance values. However, deposition of reworked vitrinites cannot be excluded, as was also described for the thermochronological dataset of Fosdick *et al*. (2014), and over-estimation for Oligocene and Neogene vitrinite reflectance values is therefore possible.

DISCUSSION

Comparison of the burial, temperature and maturation histories for the different well locations modelled in the Austral Basin indicate both similarities and differences. The highest source rock maturities occur in the southern part of the basin, where the stratigraphic column is thickest and where the deepest burial took place. A general decrease of maturity occurs to the north and east of the basin. This maturation trend corresponds to the general geometry of the basin, which shallows to the north and east. Except for the southernmost area and the area around well 4 where a transformation ratio of 100 % was reached in the Late Cretaceous (73 Ma) or Paleocene (60 Ma), two main phases of petroleum generation are observed. The first generation phase started in the Late Cretaceous and corresponds to the deep burial of the source rock intervals. The onset of the Andean orogeny in the Turonian, and the increased sediment supply resulting from Andean uplift and erosion during the Late Cretaceous, was responsible for progressive burial together with initial petroleum generation. A palaeo temperature maximum was reached at the end of the Late Cretaceous. Palaeo temperatures then increased or decreased with respect to further burial (southern and western areas) or uplift (central and northern areas) during the Paleocene and Eocene. Since the Oligocene, renewed burial occurred throughout the basin and resulted in maximum burial in the Miocene (6 Ma). This deep burial coexisted with a progressive migration of volcanism to the south during the Early Cenozoic and maximum volcanic activity in the Early to Late Miocene in Patagonia (Ramos *et al*., 1982). Increased heat flow values since the end of the Oligocene resulted in a second pulse of petroleum generation in the Miocene. Dikes and an intrusion (dated e.g. by Kay *et al*., 2004; Bruni *et al*., 2008) which are marked in Fig. 4 are located close to the Paso Fuhr area and provide evidence of increased heat flow values. The occurrence of volcanics and basaltic flows throughout the study area, and especially in the SE where the Pali Aike volcanic field is located, is supported by previous studies (e.g. Kay *et al*., 2004; Ross *et al*., 2011; Bruni *et al*., 2008) and recent seismic interpretations (Sachse *et al*., 2015).

Cycles of glaciation and deglaciation occurred since the Late Miocene in Tierra del Fuego and Patagonia (Rabassa *et al*., 2005). Ice sheet loading results in decreased temperatures in the uppermost crustal layers; uplift and surface erosion occurs during interglacials. The impact of ice loading was not determined in this study but may be considered in more detailed modelling in future.

The Malvinas Basin has a decoupled tectonic history compared to the Austral Basin. At least since the Miocene, sediment accumulation in the Malvinas Basin exceeded that of the Austral Basin. The main source for these sediments was the Fuegian Andes (Baristeas *et al*., 2012; Sachse *et al*., 2015). Thus, the

second phase of petroleum generation is closely associated with the sediment supply from the Fuegian Andes. Based on the elevated heat flow values (Fig. 7), the thermal influence of e.g. the Pali Aike Volcanic Field (Fig. 1B) on the thermal history of the Malvinas Basin cannot be excluded. Furthermore, higher palaeo heat flow values in the easternmost part of the study area are likely to be related to rift phases in the south of the basin since the Jurassic.

The results of maturity and transformation ratio modelling match with exploration results in both basins: the western Malvinas Basin does not host any significant petroleum accumulation, in contrast to the Austral Basin where a number of accumulations have been discovered. As most of the "prominent" accumulations (i.e. Carina, Aries and Condor) are located on the western flank of the Rio Chico High, in an area where maturities are marginal oil window, petroleum migration from the inner, mature parts of the Austral Basin is highly likely to have occurred. However migration from the Malvinas Basin will not be significant because both of the low maturities of the potential source rocks there and also because the Rio Chico High will act as a "barrier" to fluid flow.

CONCLUSIONS

The petroleum systems model presented here indicates two major phases of hydrocarbon generation in the Austral Basin and the westernmost part of the Malvinas Basin. The first generation phase is related to subsidence-related burial in the Late Cretaceous due to foreland flexure, with sediment supply from the uplifting and eroding Andes in the west. A second generation phase is related to a later phase of deep burial in the Miocene; a Miocene volcanic episode also influenced this phase in the Austral Basin. However, the magmatically-induced increased heat flow values are local and do not seem to have affected the whole of the study area. The volcanic rocks may have influenced the thermal history and thus hydrocarbon composition (due to degradation processes), as well as migration behavior and reservoir characteristics, as described for other basin systems worldwide.

Basin analysis based on maturity data indicates that erosion has had only a minor effect on organic matter maturation and petroleum generation, except for the Paso Fuhr area where Neogene erosion was significant and eroded thicknesses of up to 1000 m can be assumed.

The magnitude and lateral extent of the magmatically-induced Miocene heat flow have to be taken into account. The present model is based on the assumption of deepest burial and maximum temperatures reached during the Miocene, but an earlier onset of uplift and erosion (e.g. Late Eocene/ Oligocene) is also possible.

The results for the western Malvinas Basin suggested increasing maturity (to early oil zone maturities). As in the Austral Basin, there were two petroleum generation phases – Late Cretaceous and late Miocene – but during neither of them were maturities sufficient for significant petroleum generation to have occurred. Because the Fuegian Andes acted as the main sediment source for the Malvinas Basin at least since the Miocene, enhanced petroleum generation due to increased sediment accumulation and deeper burial is likely in the deepest parts of this basin. A scenario of increased heat flow as shown for the Austral Basin cannot be proven, due to missing data concerning the volcanic activity of this area.

This basin-scale model has quantified the burial, temperature, maturation and timing of petroleum generation histories of the Austral and western Malvinas Basins, and provides a context within which to explain the exploration failures and successes in these two basins as a consequence of variations in petroleum charge.

ACKNOWLEDGEMENTS

This study was funded by the German Research Foundation (DFG) within the priority program SPP 1375 - SAMPLE. R. Lutz (BGR), H. Villas (GeoLab Sur SA) and M. Cagnolatti (Petrobras Argentina) are thanked for constructive comments during Journal review which helped to improve the manuscript. E. Rossello

(University of Buenos Aires) is acknowledged for supporting the field work carried out in 2011. We thank Petrobras Argentina S.A. for providing important well data and allowing publication of the results.

REFERENCES

ALLEN, P.A. and ALLEN, J.R., 2013. Basin Analysis. Principles and application to petroleum play assessment. Wiley-Blackwell, London, 642pp.

BARISTEAS, N., ANKA, Z., DI PRIMIO, R., RODRIGUEZ, J.F., MARCHAL, D., and DOMINGUEZ, F., 2012. Distribution of hydrocarbon leakage indicators in the Malvinas Basin, offshore Argentine continental margin. *Marine Geology*, **332-334**, 56-74.

BARISTEAS, N., ANKA, Z., DI PRIMIO, R., RODRIGUEZ, J.F., MARCHAL, D. and DOMINGUEZ, F., 2013. New insights into the tectono-stratigraphic evolution of the Malvinas Basin, offshore of the southernmost Argentinean continental margin. *Tectonophysics*, **604**, 280-295.

BIDDLE, K.T., ULIANA, M.A., MITCHUM Jr., R.M., FITZGERALD, M.G. and WRIGHT, R.C., 1986. The stratigraphy and structural evolution of the central and eastern Magallanes Basin, southern South America. *International Association of Sedimentologists, Special Publication*, **8,** 41-61.

BRUNI, S., D'ORAZIO, M., HALLER, M.J., INNOCENTI, F., MANETTI, P., PÉCSKAY, Z. and TONARINI, S., 2008. Time evolution of magma sources in a continental back-arc setting: the Cenozoic basalts from Sierra de San Bernardo (Patagonia, Chunut, Argentina). *Geological Magazine,* **145**, 5, 714-732.

BURNHAM, A.K., BRAUN, R.L., GREGG, H.R. and SAMOUN, A.M., 1987. Comparison of methods for measuring kerogen pyrolysis rates and fitting kinetic parameters. *Energy and Fuels*, **1,** 6, 452- 458.

CAGNOLATTI, M., MARTINS, R. and VILLAR H.J., 1996. La Formación Lemaire como probable generadora de hidrocarburos en el área Angostura, Provincia de Tierra del Fuego, Argentina. *XIII° Congreso Geológico Argentino y III° Congreso de Exploración de Hidrocarburos, Buenos Aires, Actas*, **1**, 123-139.

COOLES, G.P., MACKENZIE, A.S. and QUIGLEY, T.M., 1986. Calculation of petroleum masses generated and expelled from source rocks. In: Advances in Organic Geochemistry 1985 (Eds: LEYTHAEUSER, D. and RULLKÖTTER, J.), pp. 235-245. Pergamon Press, Oxford.

DESSORT, D., CONNAN, J., DERENNE, S. and LARGEAU, C., 1997. Comparative studies of the kinetic parameters of various algaenans and kerogens via open system pyrolysis. *Organic Geochemistry*, **26**, 11-12, 705-720.

DIRAISON, M., COBBOLD, P.R., GAPAIS, D., ROSSELLO, E.A., and LE CORRE, C., 2000. Cenozoic crustal thickening, wrenching and rifting in the foothills of the southernmost Andes. *Tectonophysics*, **316**, 91-119.

DOW, W. G., 1977. Kerogen studies and geological interpretations. *Journal of Geochemical Exploration*, **7,** 77-99.

ESPITALIÉ, J., UNGERER, P., IRWIN, I. and MARQUIS, F., 1988. Primary cracking of kerogens; experimenting and modeling C_1, C_2-C_5, C_6-C_{15} and C_{15+} classes of hydrocarbons formed. In: MATAVELLI, L. and NOVELLI, L., (Eds), Advances in Organic Geochemistry (1987) Part II: Analytical Geochemistry. *Organic Geochemistry,* **14**, 4-6, 893-899.

FOSDICK, J.C., GROVE, M., GRAHAM, S.A., HOURIGAN, J.K., LOVERA, O., and ROMANS, B.W., 2014. Detrital thermochronologic record of burial heating and sediment recycling in the Magallanes foreland basin, Patagonian Andes. *Basin Research,* 1-27.

FRANZESE, J., SPALLETTI, L., GÓMEZ PÉREZ and MACDONALD, D., 2003. Tectonic and paleoenvironmental evolution of Mesozoic sedimentary basins along the Andean foothills of Argentina (32°–54°S). *Journal of Earth Sciences,* **16**, 1, 81-90.

GALEAZZI, J. S., 1998. Structural and Stratigraphic Evolution of the Western Malvinas Basin, Argentina. *AAPG Bulletin,* **82**, **4,** 596-636.

GHIGLIONE, M.C., 2002. Diques clásticos asociados a deformación transcurrente en depósitos sinorogénicos del Mioceno inferior de la Cuenca Austral. *Revista de la Asociación Geológica Argentina*, **57**, 2, 103-118.

GHIGLIONE, M.C., SUAREZ, F., AMBROSIO, A., DA POIAN, G., CRISTALLINI, E.O., PIZZIO, M.F. and REINOSO, R.M., 2009. Structure and evolution of the Austral Basin fold-thrust belt, southern Patagonian Andes. *Revista de la Asociación Geolóica Argentina,* **65**, 1, 215-226.

GHIGLIONE, M.C., QUINTEROS, J., YAGUPSKY, D., BONILLOMARTÍNEZ, P., HLEBSZEVTICH, J., AMOS, V.A., VERGANI, G., FIGUEROA, D., QUESADA, S. and ZAPATA, T., 2010. Structure and tectonic history of the foreland basins of southernmost South America. *Journal of South American Earth Sciences*, **29**, 2, 262-277.

HANTSCHEL, T. and KAUERAUF, A. I., 2009. Fundamentals of Basin and Petroleum Systems Modeling. Springer Verlag, Berlin, 476 pp.

HINTERWIMMER, G., 2002. Los reservorios de la Serie Tobífera, in M. Schiuma, G. Hinterwimmer and G. Vergani, eds., Rocas reservorio de las cuencas productivas de la Argentina: Simposio del V Congreso de Exploración y Desarrollo de Hidrocarburos, Mar del Plata, Buenos Aires, Instituto Argentino del Petróleo y del Gas, 27-47.

HUBBARD, S.M., ROMANS, B.W. and GRAHAM, S.A., 2007. An outcrop example of large-scale conglomeratic intrusions sourced from deep-water channel deposits, Cerro Toro Formation, Magallanes basin, southern Chile. In: Hurst, A. and Cartwright, J., (Eds), Sand injectites: Implications for hydrocarbon exploration and production. *AAPG Memoir,* **87**, 199-207.

KAY, S.M., GORRING, M. and RAMOS, V. A., 2004. Magmatic sources, setting and causes of Eocene to Recent Patagonian plateau magmatism (36°S to 52°S latitude). *Revista de la Asociación Geológica Argentina*, **59**, 4, 556-568.

MARINELLI, R., 1998. Reservorios deltaicos de la Formatión Piedra Clavada. *Boletín de Informaciones Petroleras*, **15**, 28-37.

NATALND, M.L., GONZALEZ, P.E., CANON, A. and ERNST, M., 1974. A system of stages for correlation of Magallanes Basin sediments. *AAPG Memoir,* **139**, 126.

OLIVERO, E.B. and MARTINIONI, D.R., 2001. A review of the geology of the Fuegian Andes. *Journ. South American Earth Sciences,* **14,** 2, 175-188.

OlLIVERO, E.B. and MALMUIÁN, D.R., 2008. Mesozoic- Cenozoic stratigraphy of the Fuegian Andes, Argentina. *Geologica Acta,* **6**, 1, 5-18.

ORTIZ-JAUREGUIZAR, E. and CLADERA, G. A., 2006. Paleoenvironmental evolution of southern South America during the Cenozoic. *Journal of Arid Environments,* **66**, 3, 498-532. PEPPER, A. S. and CORVI, P. J. 1995. Simple kinetic models of petroleum formation: Part I Oil and gas generation from kerogen. *Marine and Petroleum Geology*, **12,** 3, 291-319.

PITTION, J. L. and GOUADAIN, J., 1992. Source rocks and oil generation in the Austral basin. Acts of the Thirteenth World Petroleum Congress, Buenos Aires, *Proceedings* **2,** 113-120. PITTION, J.L. and ARBE, H.A., 1999. Sistema petrolero de la Cuenca Austral. IV Congreso Exploración y desarrollo de hidrocarburos, Mar del Plata, *Actas* **I**, 239-262.

POELCHAU, H.S., BAKER, D.R. HANTSCHEL, T., HORSFIELD, B. and WYGRALA, B., 1997. Simulation and the design of the conceptual basin model. In: WELTE, D.H., HORSFIELD, B. and BAKER, D.R. (Eds), Petroleum Basin Evolution. Springer Verlag, Berlin, 3-70.

RABASSA, J., CORONATO, A.M. and SALEMME, M., 2005. Chronology of the Late Cenozoic Patagonian glaciations and their correlation with biostratigraphic units of the Pampean region (Argentina). *Journal of South American Earth Science*, **20**, 81-103.

RAMOS, V.A., 1989. Andean foothills structures in Northern Magallanes Basin, Argentina. *AAPG Bull*. **73**, 7, 887-903.

REYNOLDS, J.G., and BURNHAM, A.K., 1995. Comparison of kinetic analysis of source rocks and kerogen concentrates. *Organic Geochemistry*, **23**, 1, 11-19.

ROBBIANO, J.A., ARBE, H. and GANGUI, A., 1996. Cuenca Austral Marina. Relatorio XIII Congreso Geológico Argentino y III Congreso de Exploración de Hidrocarburos, 331–341.

RODRIGUEZ, J.F. and LITTKE, R., 2001. Petroleum generation and accumulation in the Golfo San Jorge Basin, Argentina: a basin modeling study. *Marine and Petroleum Geology*, **18**, 995-1028.

RODRIGUEZ, J.F., MILLER, M. and CAGNOLATTI, M. J. ,2008. Sistemas Petroleros de Cuenca Austral, Argentina y Chile. In: Simposio: “Sistemas Petroleros de las Cuencas Andinas (Eds: C. E. Cruz, J. F. Rodríguez, J. J. Hechem and H. J. Villar). Instituto Argentino del Petróleo y del Gas. Talleres Trama S.A., Buenos Aires, 1-31.

ROSS, P.-S., DELPIT, S., HALLER, M.J., NÉMETH, K., and CORBELLA, H., 2011. Influence of the substrate on maar-diatreme volcanoes- An example of a mixed setting from the Pali Aike volcanic field, Argentina. *Journal of Volcanology and Geothermal Research,* **201**, 1-4, 253-271.

ROSSELLO, E.A., HARING, C.E., CARDINALI, G., LAFFITTE, G.A., and NEVISTIC, A.V., 2008. Hydrocarbons and petroleum geology of Tierra del Fuego, Argentina. *Geologica Acta*, **6,** 1, 69-83.

RULLKÖTTER, J., LEYTHAEUSER, D., HORSFIELD, B., LITTKE, R., MANN, U., MÜLLER, P.J., RADKE, M., SCHAEFFER, R., SCHENK, H.-J., SCHWOCHAU, K., WITTE, E.G., WELTE, D.H., 1987. Organic matter maturation under influence of a deep intrusive heat source: A natural experiment for quantitation of hydrocarbon generation and expulsion from a petroleum source rock (Toarcian shale, northern Germany). *Organic Geochemistry*, **13,** 4-6, 847-856.

SACHSE, V.F., STROZYK, F., ANKA, Z., RODRIGUEZ, J.F., and DI PRIMIO, R., 2015. The tectonostratigraphic evolution of the Austral Basin and adjacent areas against the background of Andean tectonics, southern Argentina, South America. *Basin Research,* DOI: 10.1111/bre.12118.

SCHENK, H.J. and DIECKMANN, V. 2004. Prediction of petroleum formation: the influence of laboratory heating rates on kinetic parameters and geological extrapolations. *Marine and Petroleum Geology*, **21**, 1, 79-95.

SENGLAUB, Y., LITTKE, R., and BRIX, M.R., 2006. Numerical modelling of burial and temperature history as an approach for an alternative interpretation of the Bramsche anomaly, Lower Saxony Basin. *International Journal of Earth Sciences,* **95**, 204-224.

SRUOGA, P., and RUBINSTEIN, N., 2002. Procesos deutéricos y diagenéticos en volcanitas de la provincia Chon-Aike, Santa Cruz, Argentina. Implicancias en el desarrollo de la porosidad y permeabilidad. Actas del XV Congreso Geológico Argentino, 2, 9-14.

SRUOGA, P., RUBINSTEIN, N., and HINTERWIMMER, G., 2004. Porosity and permeability in volcanic rocks: a case study on the Serie Tobífera, South Patagonia, Argentina. *Journal of Volcanology and Geothermal Research*, **132**, 1, 31-43.

SRUOGA, P., and RUBINSTEIN, N., 2007. Processes controlling porosity and permeability in volcanic reservoirs from the Austral and Neuquén Basins, Argentina. *AAPG Bulletin*, **91**, 1, 115-129.

SUÁREZ, M., DE LA CRUZ, R., and BELL, C.M., Timing and origin of deformation along the Patagonian fold and thrust belt. Geological Magazine, 137, 4, 345-353. SWEENEY, J.J., and BURNHAM, A.K., 1990. Evaluation of a simple model of vitrinite reflectance based on chemical kinetics. *AAPG Bulletin*, **74**, 10, 1559-1570.

TASSONE, A., LODOLO, E., MENICHETTI, M., YAGUPSKY, D., CAFFAU, M., and VILAS, J.F., 2008. Seismostratigraphic and structural setting of the Malvinas Basin and its southern margin (Tierra del Fuego Atlantic offshore). *Geologica Acta*, **6,** 55-67.

THOMAS, C.R., 1949. Geology and Petroleum Exploration in Magallanes Province, Chile. *AAPG Bulletin,* **33**, 9, 1553-1578.

UYEDA, S., WATANABE, T., KAUSEL, E., KUBO, M., and YASHIRO, Y., 1978. Report of heat flow measurements in Chile. *Bulletin of the Earthquake Research Institute*, **53**, 131-163.

VILLAR, H.J., PÜTTMANN, W. and WOLF, M., 1988. Organic geochemistry and petrography of Tertiary coals and carbonaceous shales from Argentina. *Organic Geochemistry*, **13**, 4-6, 1011-1021.

WELTE, D. H., HORSFIELD, B. and BAKER, D.R. 1997. Petroleum and Basin Evolution, Springer Verlag, Berlin, 535 pp. WELTE, D.H., and YALCIN, M.N., 1988. Basin modeling - a new comprehensive method in petroleum geology. *Organic Geochemistry,* **13,** 141-151.

WELTE, D.H., and YÜKLER, M.A. 1981. Petroleum origin and accumulation in basin evolution- a quantitative approach. *AAPG Bulletin,* **65**, 8, 1387-1396. WILSON, T.J., 1991. Transition from back-arc to foreland basin development in southernmost Andes: Stratigraphic record from the Ultima Esperanza District, Chile. *Geol. Soc. Am. Bull*., **103**, 1, 98–111.

WYGRALA, B.P., 1989. Integrated study of an oil field in the southern Po Basin, Northern Italy. PhD thesis, University of Cologne, Germany.

ZAMBRANO, J. J. and URIEN, C.M., 1970. Geological outlines of the basins in southern Argentina and their offshore extension. *Journal of Geophysical Research*, **75**, 1363–1396.

ZIELINSKI, G.W., and BRUCHHAUSEN, P. M., 1983. Shallow temperature and thermal regime in the hydrocarbon province of Tierra del Fuego. *AAPG Bulletin,* **67,** 1, 166-177.

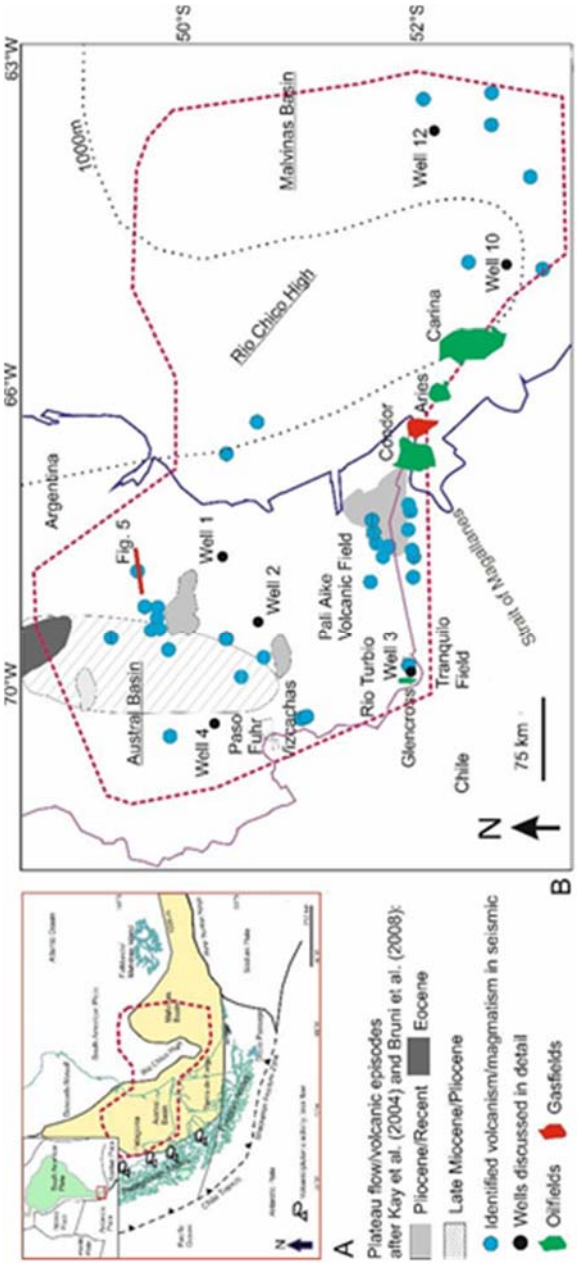

Fig. 1. A: Location map of the study area (marked by red dashed line, extent of 3D geomodel) in the offshore Austral and western Malvinas Basin, offshore SE Argentina. Modified from Sachse et al. (2015), based on data in Biddle et al. (1986), Wilson (1991) and Thomson et al. (2001). B Map of the study area in SE Argentina showing the location of the studied wells together with volcanic fields and magmatic intrusions interpreted on seismic profiles. Black dashed line represents 1000 m of sedimentary fill. The location of the cross-section in Fig. 5 is marked. The burial histories of wells 1-4 (Austral Basin) and 10, 12 (Malvinas Basin) are discussed in detail in the text under Results.

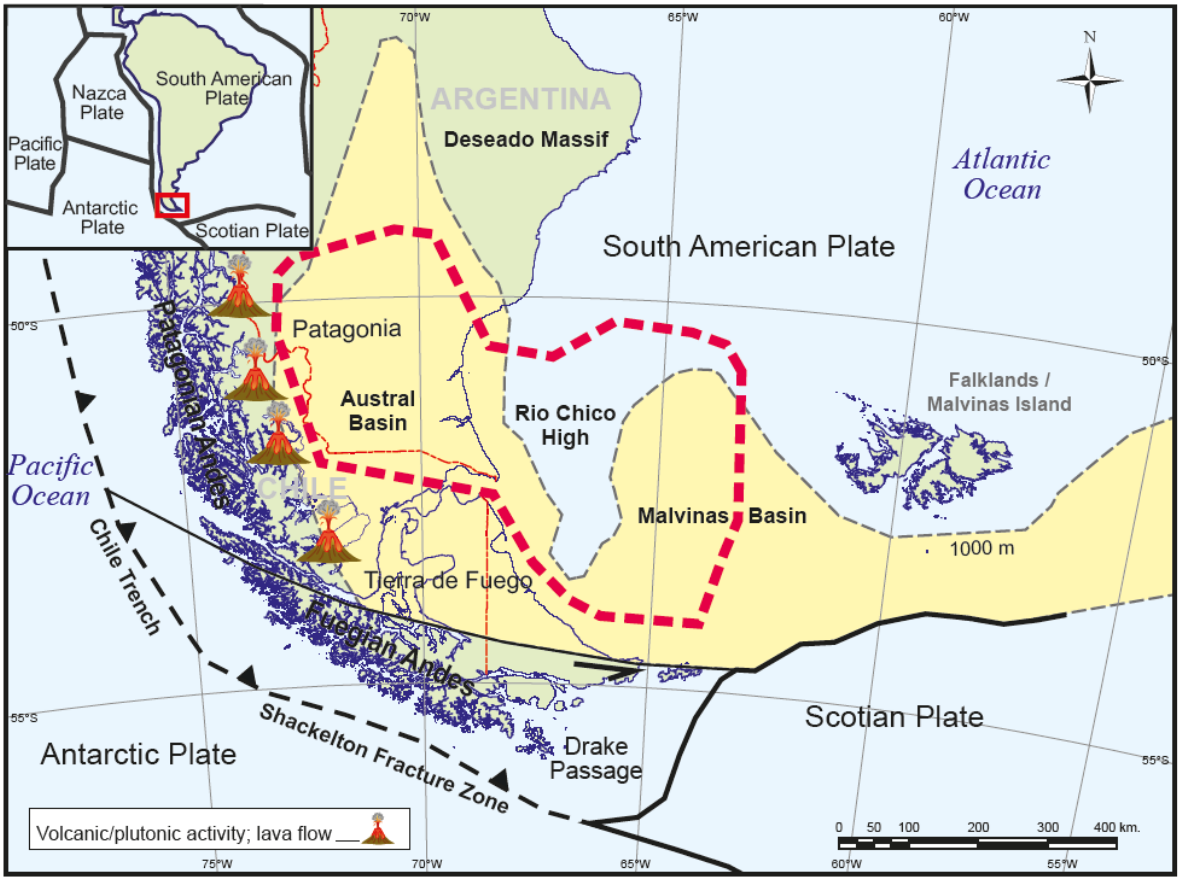
Nazca Plate
South American Plate
Pacific Plate
Antarctic Plate
Scotian Plate
ARGENTINA
Deseado Massif
Atlantic Ocean
South American Plate
Patagonia
Austral Basin
Rio Chico High
Falklands / Malvinas Island
Malvinas Basin
1000 m
Pacific Ocean
CHILE
Patagonian Andes
Chile Trench
Tierra de Fuego
Fuegian Andes
Scotian Plate
Antarctic Plate
Shackelton Fracture Zone
Drake Passage
Volcanic/plutonic activity; lava flow
0 50 100 200 300 400 km.
70°W
65°W
60°W
55°W
50°S
55°S
75°W
N

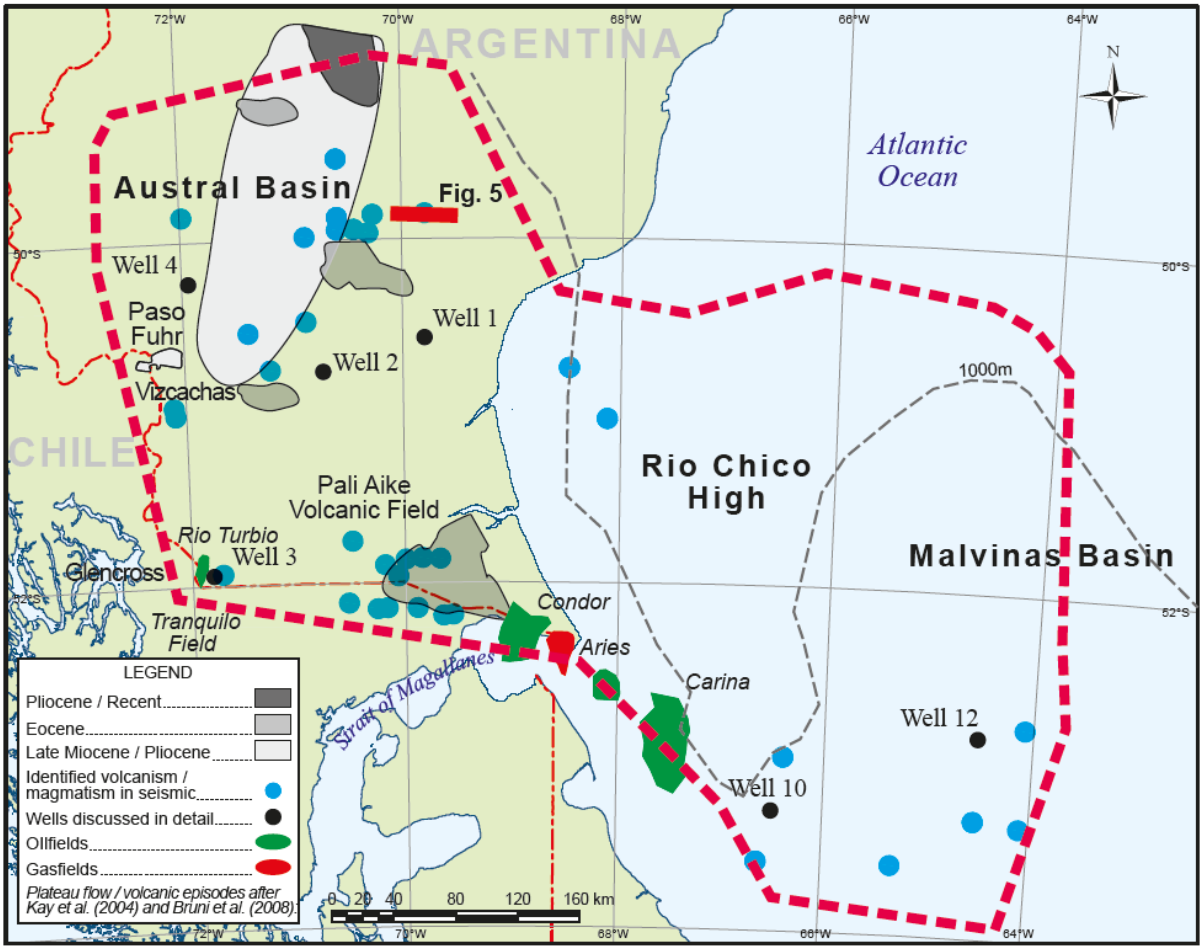
ARGENTINA
Austral Basin
Fig. 5
Atlantic Ocean
Well 4
Paso Fuhr
Well 1
Well 2
Vizcachas
CHILE
Pali Aike Volcanic Field
Rio Turbio
Well 3
Glencross
Tranquilo Field
Rio Chico High
1000m
Malvinas Basin
Condor
Aries
Carina
Strait of Magellanes
Well 12
Well 10
LEGEND
Pliocene / Recent
Eocene
Late Miocene / Pliocene
Identified volcanism / magmatism in seismic
Wells discussed in detail
Oilfields
Gasfields
Plateau flow / volcanic episodes after Kay et al. (2004) and Bruni et al. (2008).
0 20 40 80 120 160 km
72°W
70°W
68°W
66°W
64°W
50°S
52°S
N

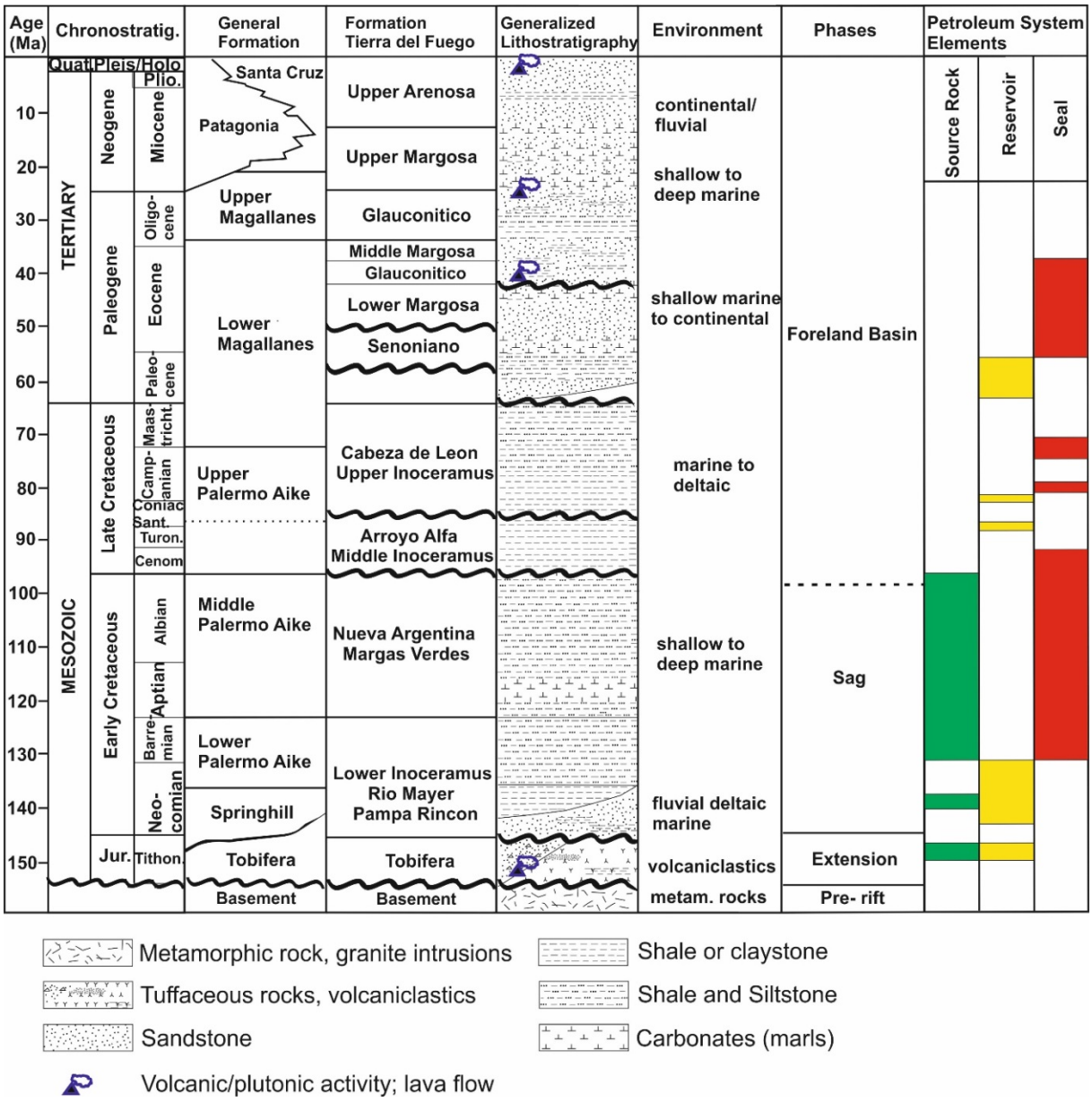

Fig. 2. Chronostratigraphic chart for the Austral Basin, showing the main tectonic phases and the petroleum system elements (modified after Sachse et al., 2015; compiled from Biddle et al., 1986; Pittion and Gouadain, 1992; Galeazzi, 1998; and Franzese et al., 2003).

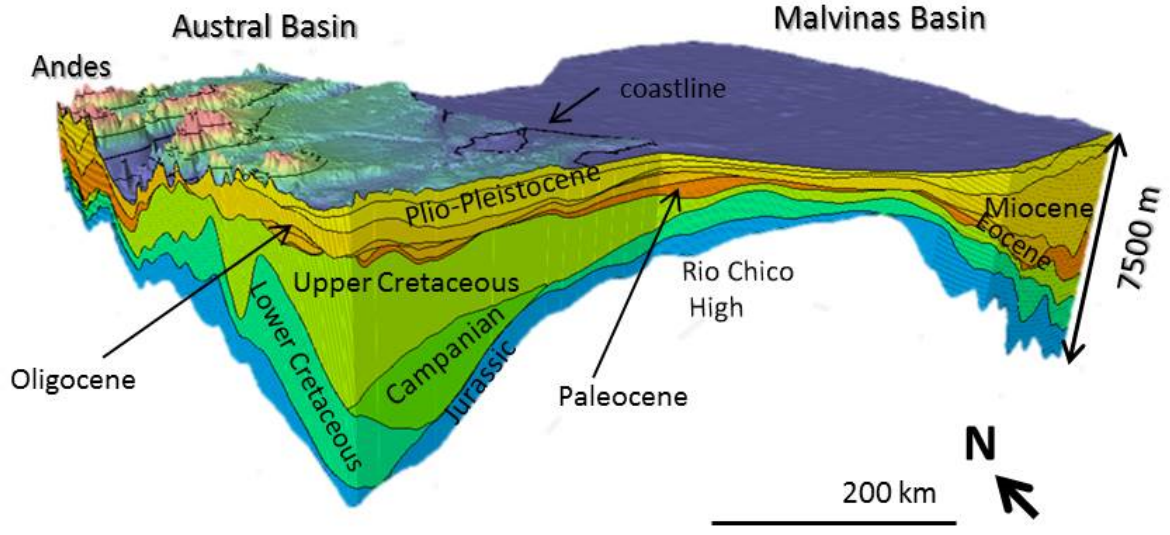

Fig. 3. 3D geomodel of the study area in the Austral and Malvinas Basins (see Fig. 1 for location) based on seismostratigraphic interpretations (Sachse et al., 2015).

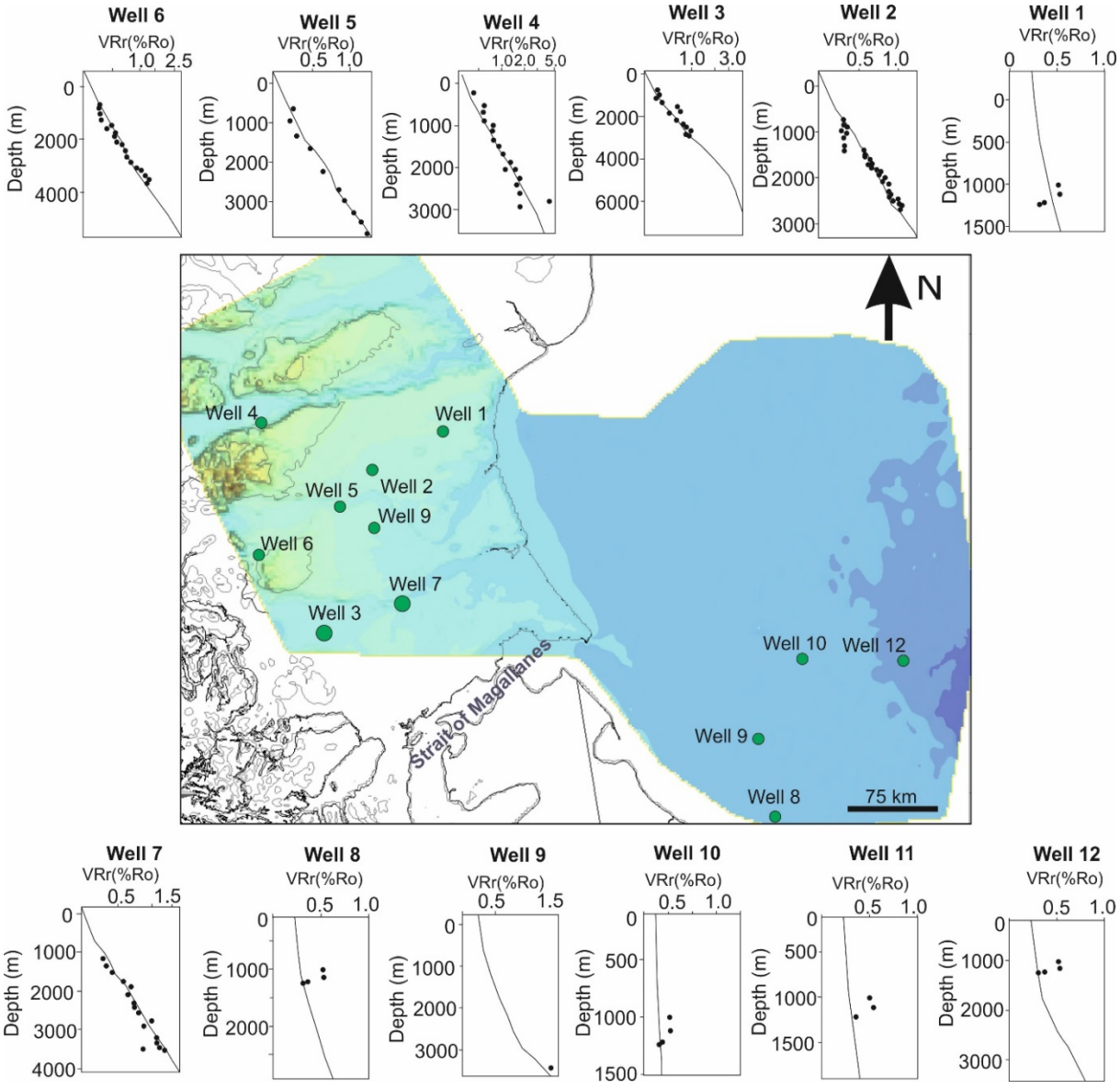

Fig. 4. Profiles of VRr versus depth showing calibration data for wells in the study area; calibration is based on a comparison of measured (dots) and calculated vitrinite reflectance data (solid line). The map shows the well locations in the study area; background colour shows topography (onshore) and bathymetry (offshore).

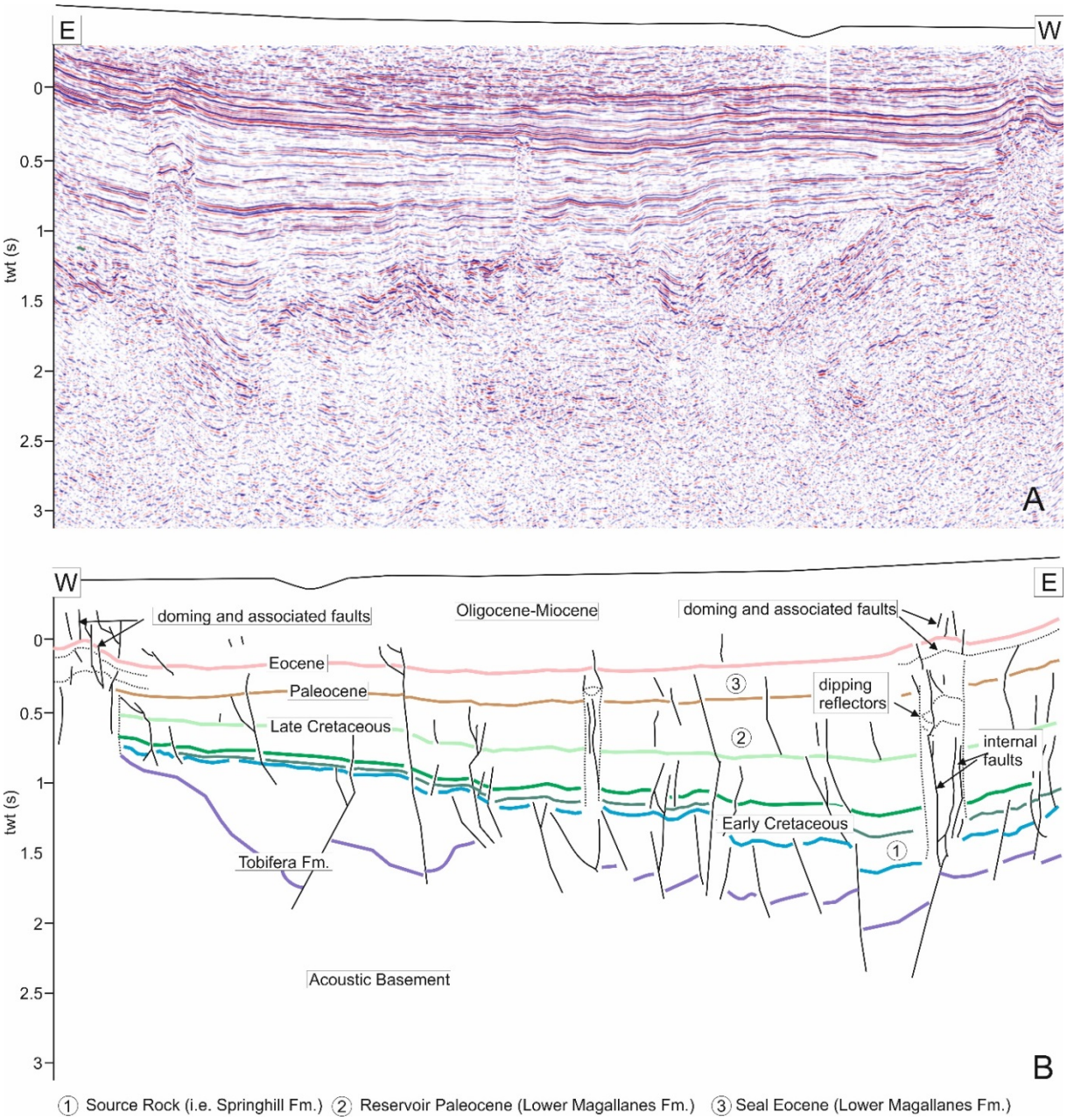

Fig. 5. Uninterpreted (A) and interpreted (B) west-east seismic profile in the northern Austral Basin (see Fig. 1B for location) showing the principal petroleum systems elements, together with faults (solid lines) and intrusion structures (dashed lines).

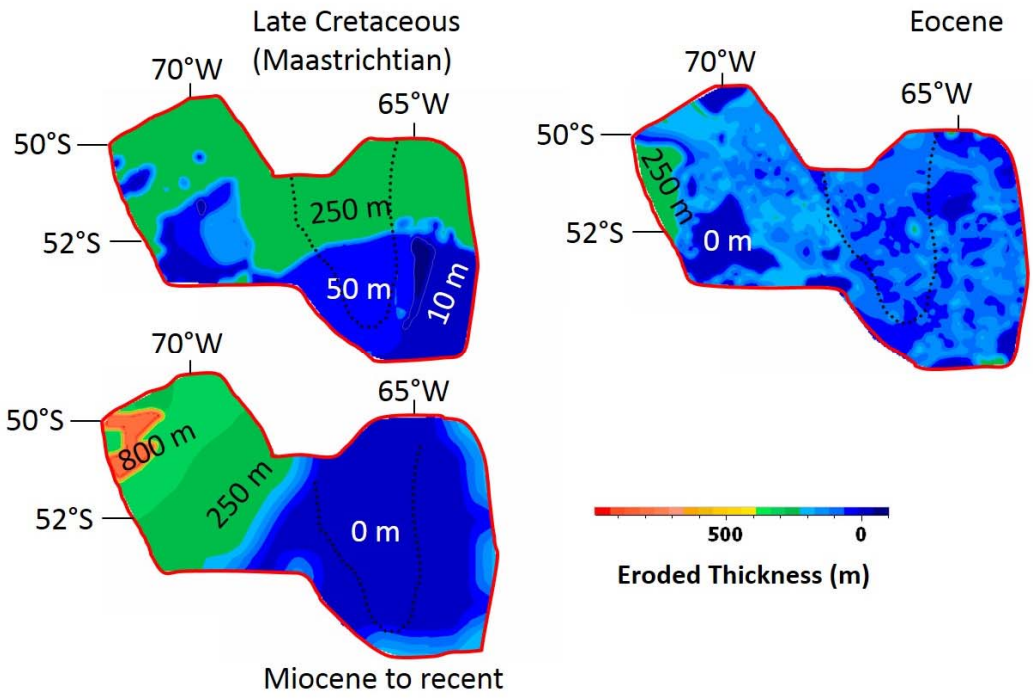

Fig. 6. Maps of the study area (see location in Fig. 1) showing eroded thicknesses for the Late Cretaceous (Maastrichtian), the Eocene, and the Miocene to -Recent erosional phases.

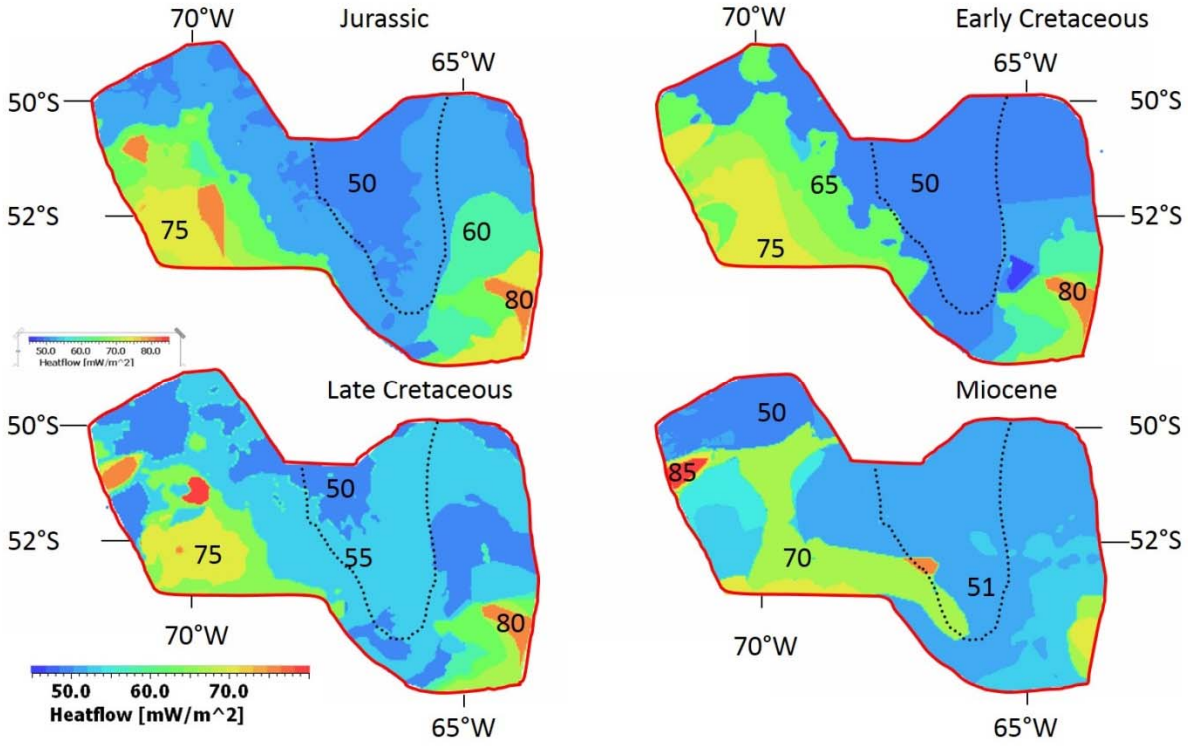

Fig. 7. Maps of the study area (see location in Fig. 1; black dashed line shows basin outlines) showing regional heat flow at four time steps (Jurassic, Early Cretaceous, Late Cretaceous, Miocene) used for calibration.

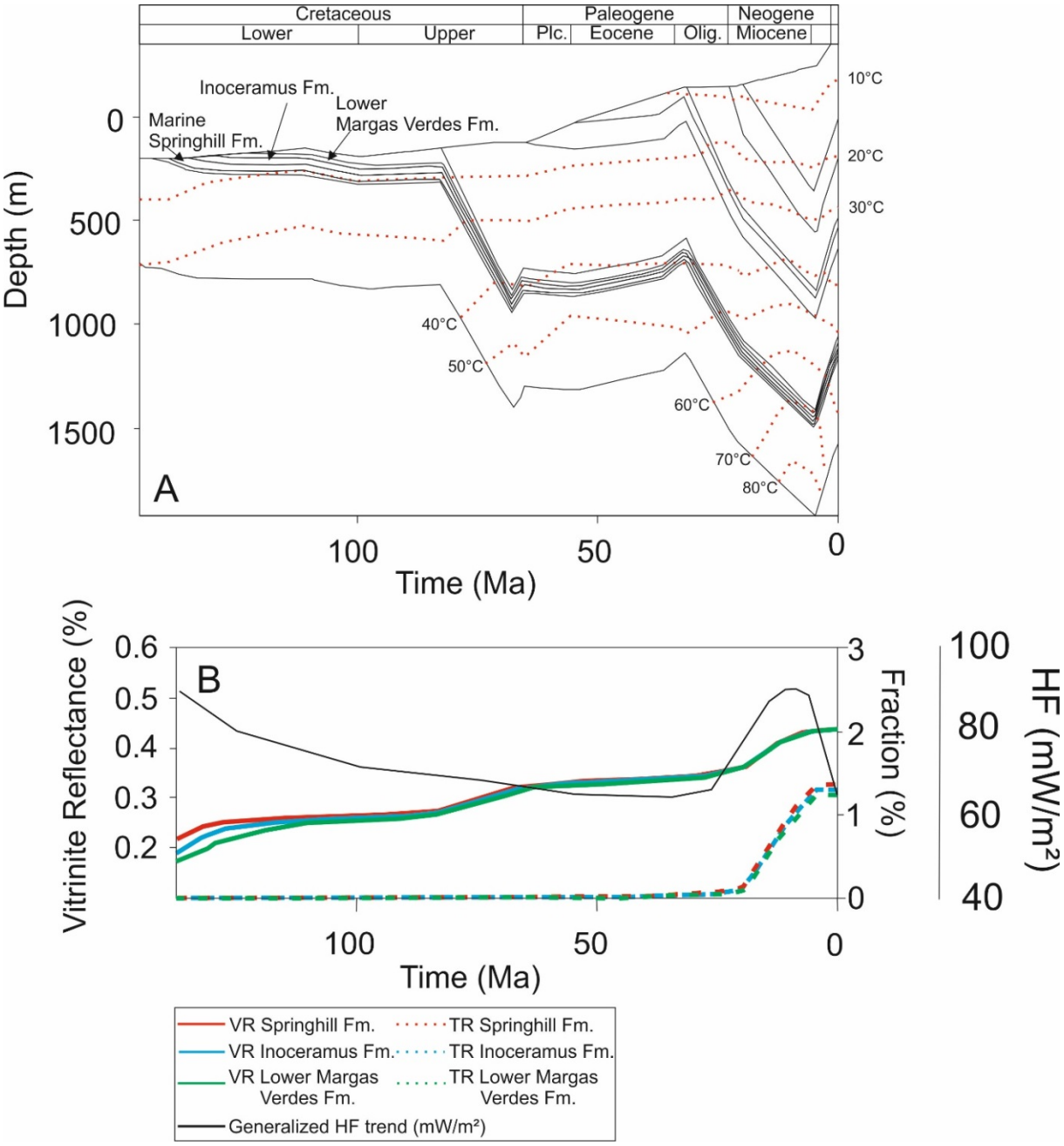

Fig. 8. A. Burial history plot including temperature isolines for well 1 in the northern Austral Basin (well location in Fig. 1; calibration curve in Fig. 4). B. Profiles show the maturation history (solid lines) and transformation ratio (dashed lines) for source rock intervals in the Lower Cretaceous Springhill, Inoceramus and Lower Margas Verdes Formations at well 1. The black line shows the generalized heat flow trend.

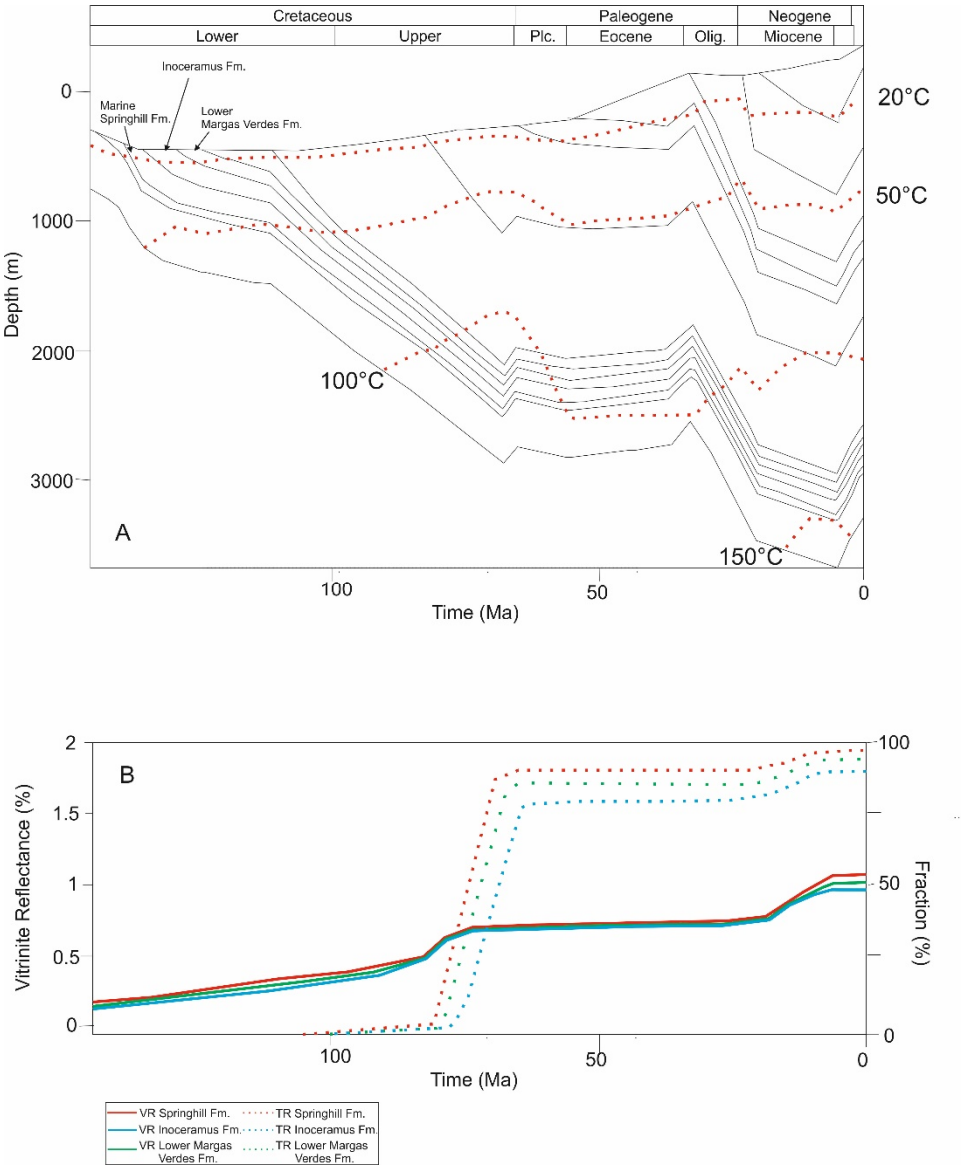

Fig. 9. A. Burial history plot including temperature isolines for well 2 in the central Austral Basin (well location in Fig. 1; calibration curve in Fig. 4). B. Profiles show the maturation history (solid lines) and transformation ratio (dashed lines) for source rock intervals in the Lower Cretaceous Springhill, Inoceramus and Lower Margas Verdes Formations at well 2.

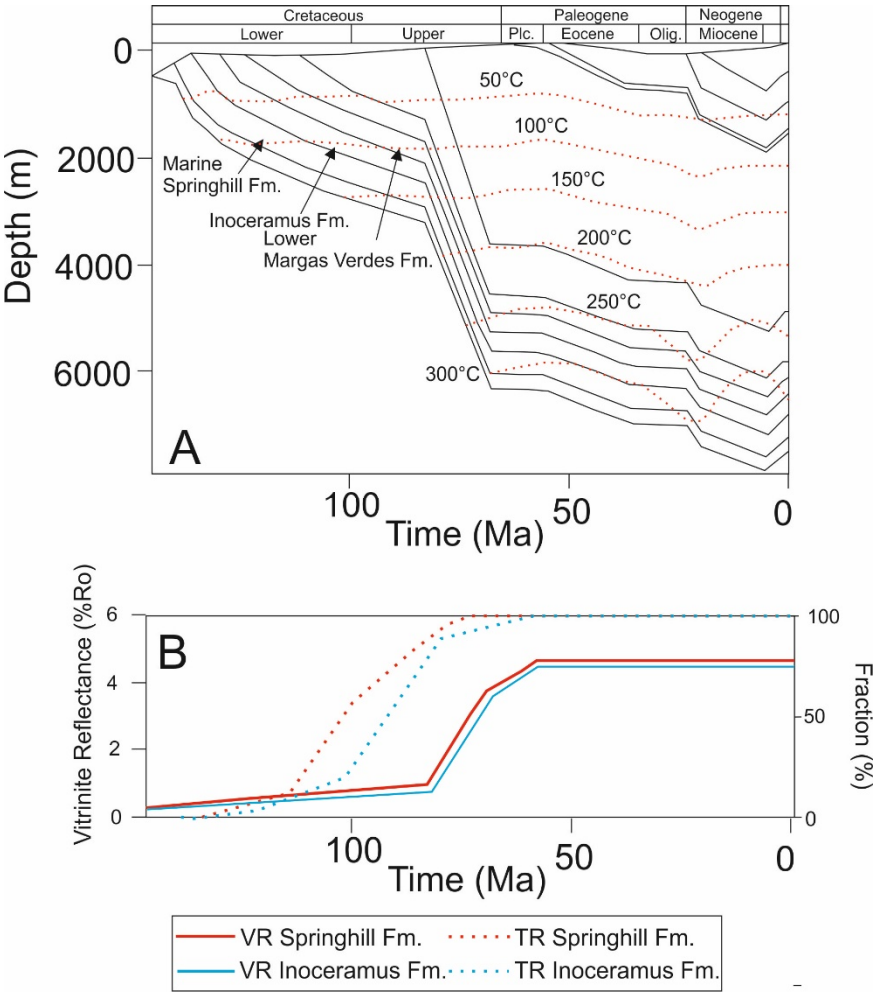

Fig. 10. A. Burial history plot including temperature isolines for well 3 in the southern Austral Basin (well location in Fig. 1; calibration curve in Fig. 4). B. Profiles show the trends of maturation history (solid lines) and transformation ratio (dashed lines) for source rock intervals in the Lower Cretaceous Springhill and Inoceramus Formations; the Lower Margas Verdes Formations was assigned as sandstone at this location.

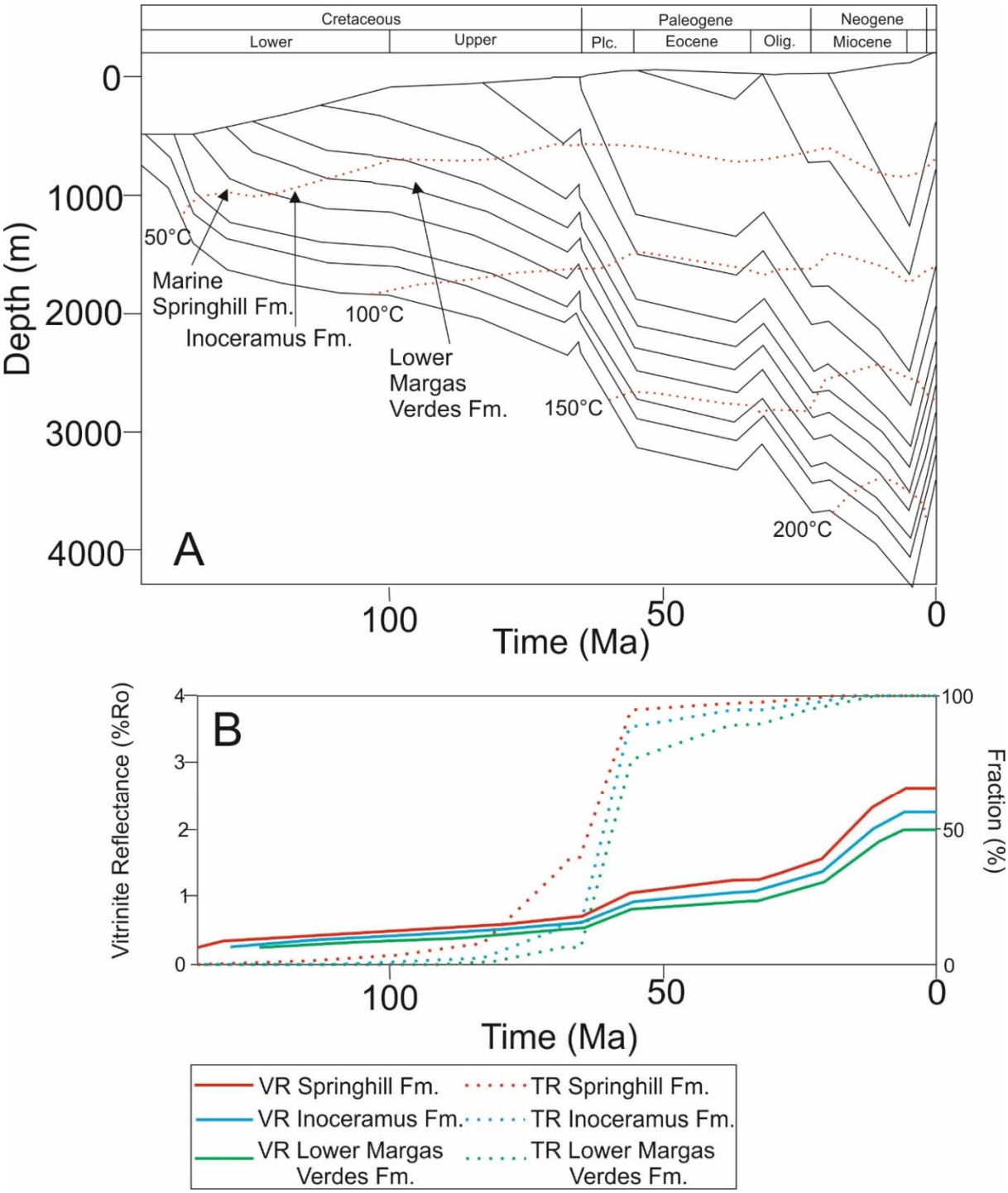

Fig. 11. A. Burial history plot including temperature isolines for well 4 in the western Austral Basin (well location in Fig. 1; calibration curve in Fig. 4). B. Profiles show the maturation history (solid lines) and transformation ratio (dashed lines) for source rock intervals in the Lower Cretaceous Springhill, Inoceramus and Lower Margas Verdes Formations at well 4.

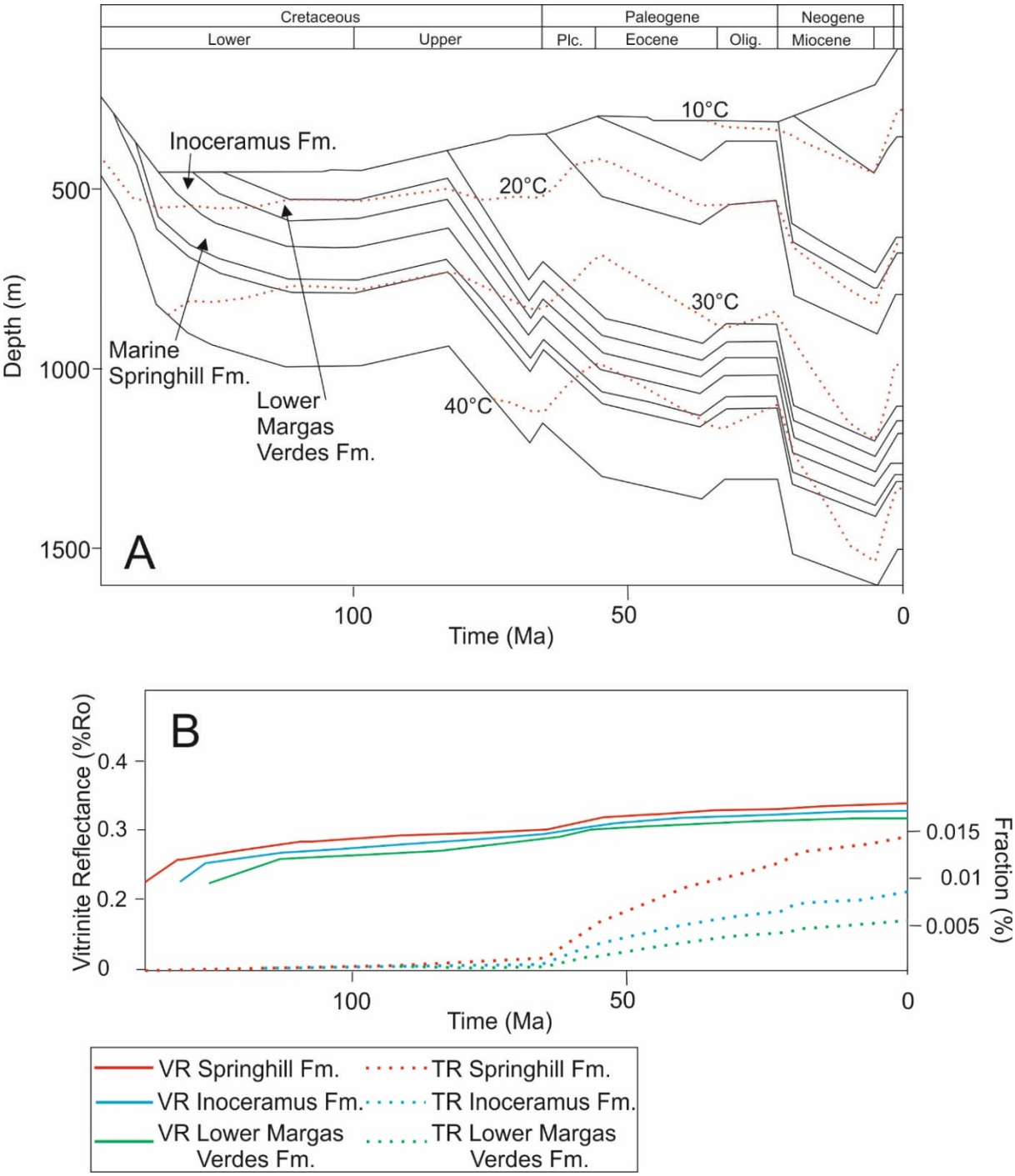

Fig. 12. A. Burial history plot including temperature isolines for well 10 in the central Malvinas Basin (well location in Fig. 1; calibration curve in Fig. 4). B. Profiles show the maturation history (solid lines) and transformation ratio (dashed lines) for source rock intervals in the Lower Cretaceous Springhill, Inoceramus and Lower Margas Verdes Formations at well 10.

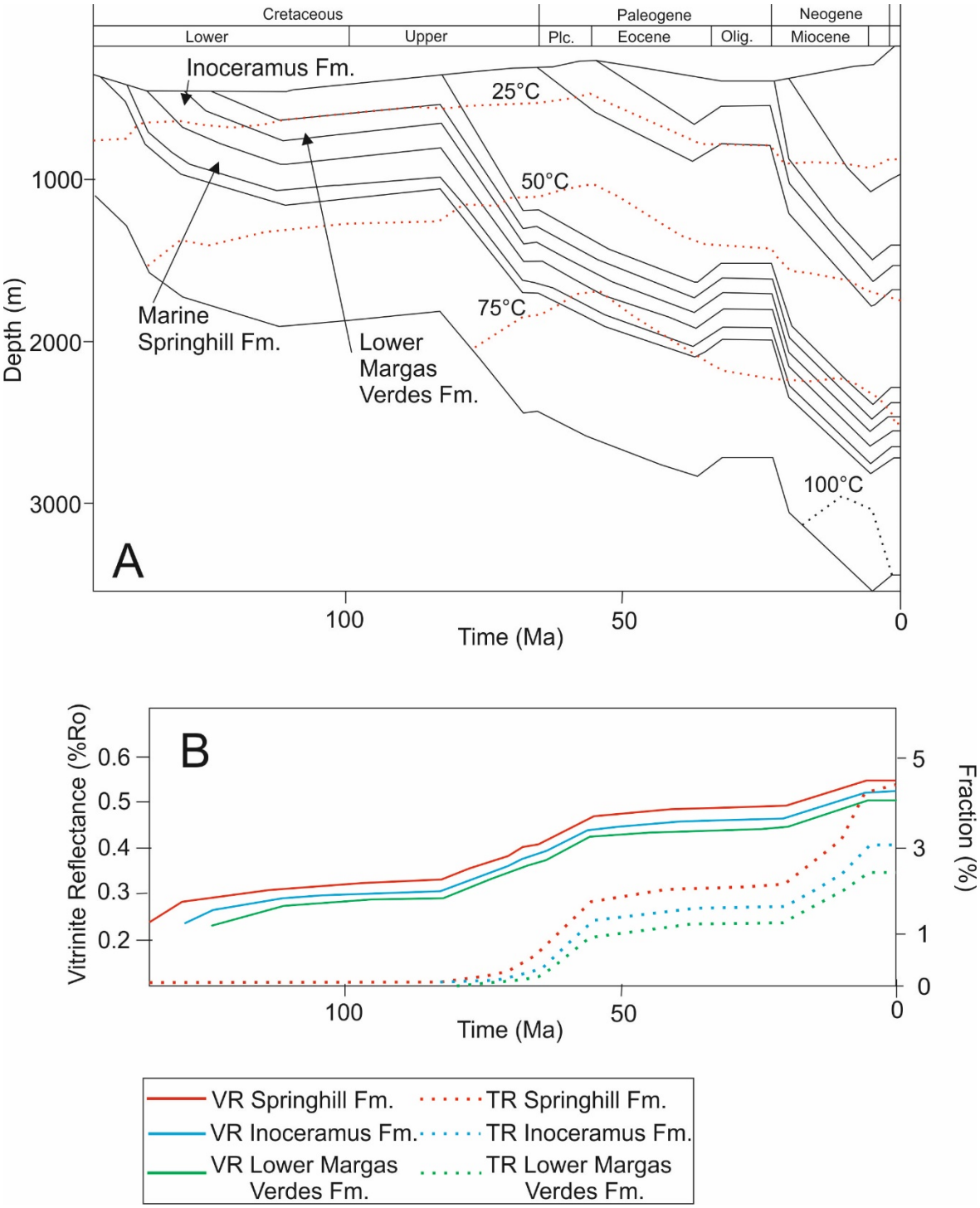

Fig. 13. A. Burial history plot including temperature isolines for well 12 in the eastern Malvinas Basin (well location in Fig. 1; calibration curve in Fig. 4). B. Profiles show the maturation history (solid lines) and transformation ratio (dashed lines) for source rock intervals in the Lower Cretaceous Springhill, Inoceramus and Lower Margas Verdes Formations at well 12.

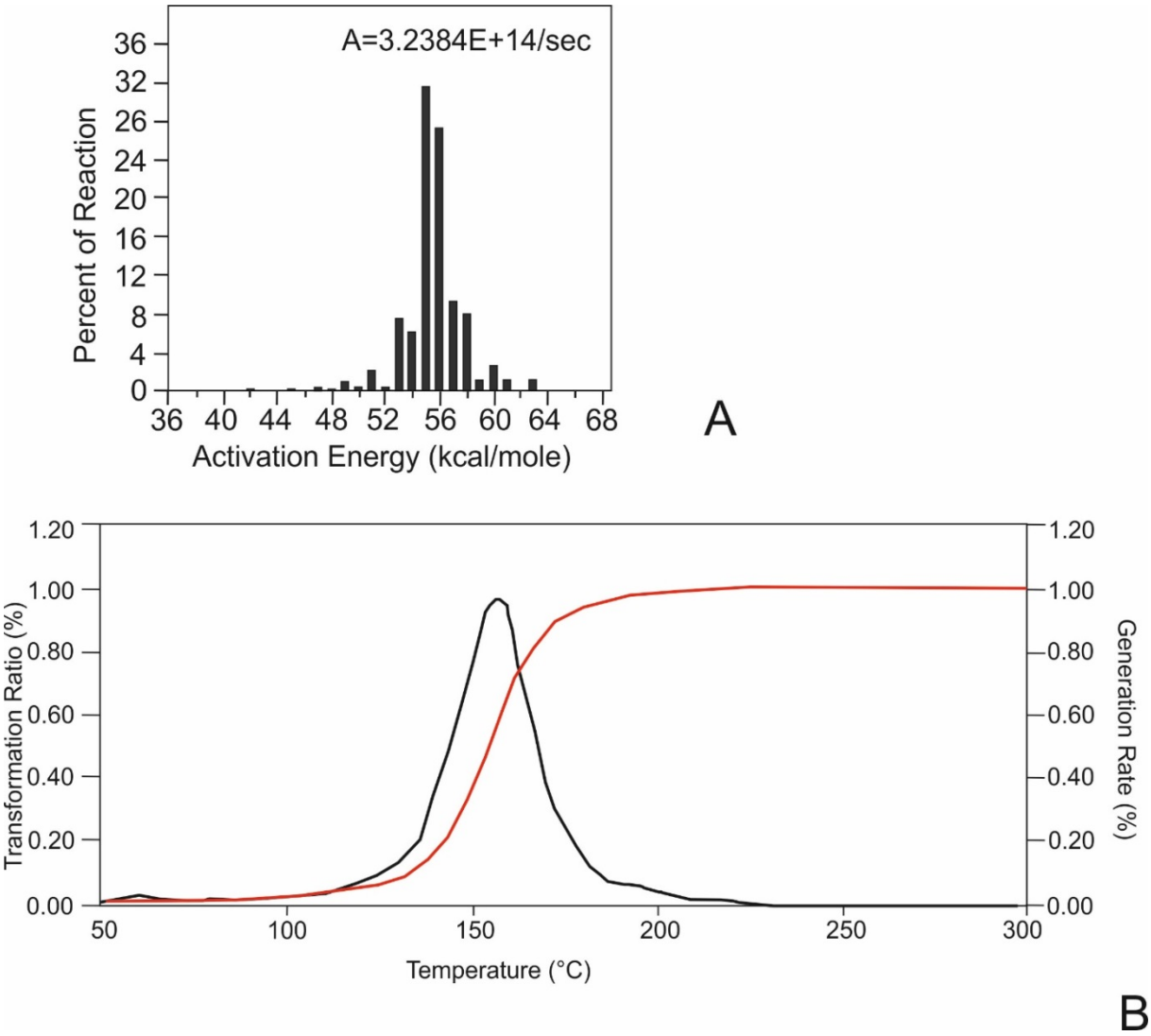

Fig. 14. Bulk kinetic parameters for a typical source rock sample from the Springhill Formation from the study area. (A) Activation energy distribution (kcal/mole) and frequency factor. (B) Calculated generation rate (normalized in %, black curve) and calculated predictions of kerogen transformation ratio (normalized in %, red curve) versus temperature for a heating rate of 3°C/Ma.

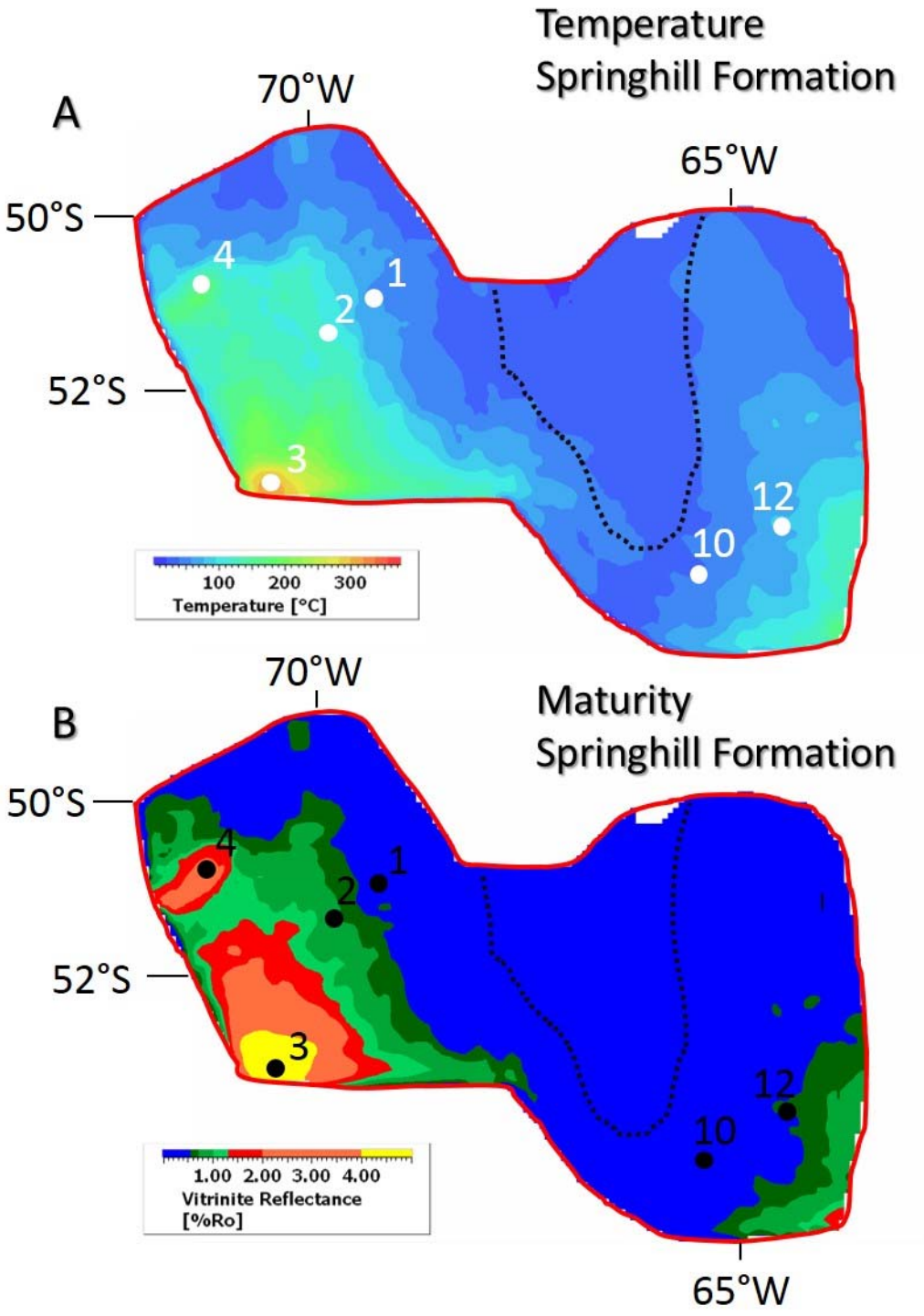

Fig. 15. Temperature (A) and maturity (B) maps for the Springhill Formation in the study area in the Austral and western Malvinas Basins. The maps for the Inoceramus and Lower Margas Verdes Formations are similar and are not therefore presented. Numbers refer to well locations (Figs. 8-13).

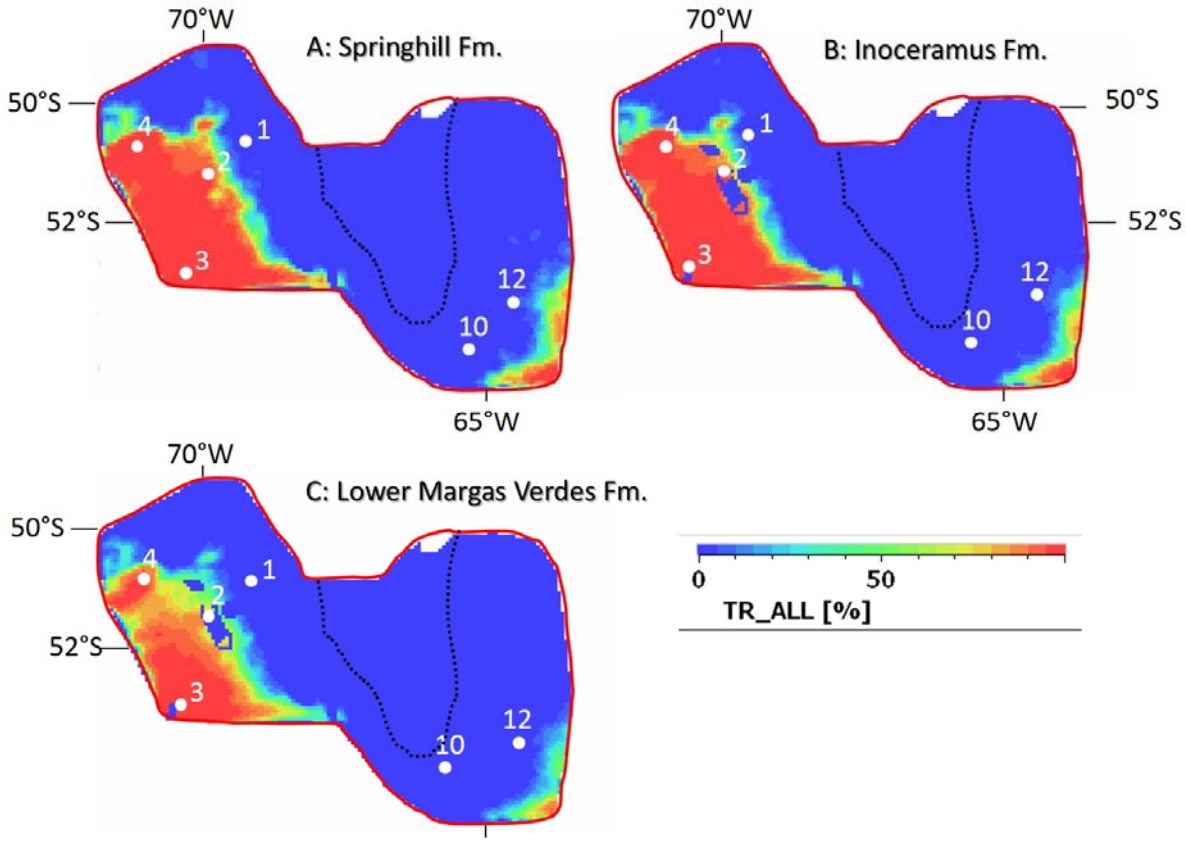

Fig. 16. Maps of the transformation ratio for the three Lower Cretaceous Springhill, Inoceramus and Lower Margas Verdes Formations in the Austral and western Malvinas Basins. Numbers refer to well locations (Figs 8-13).

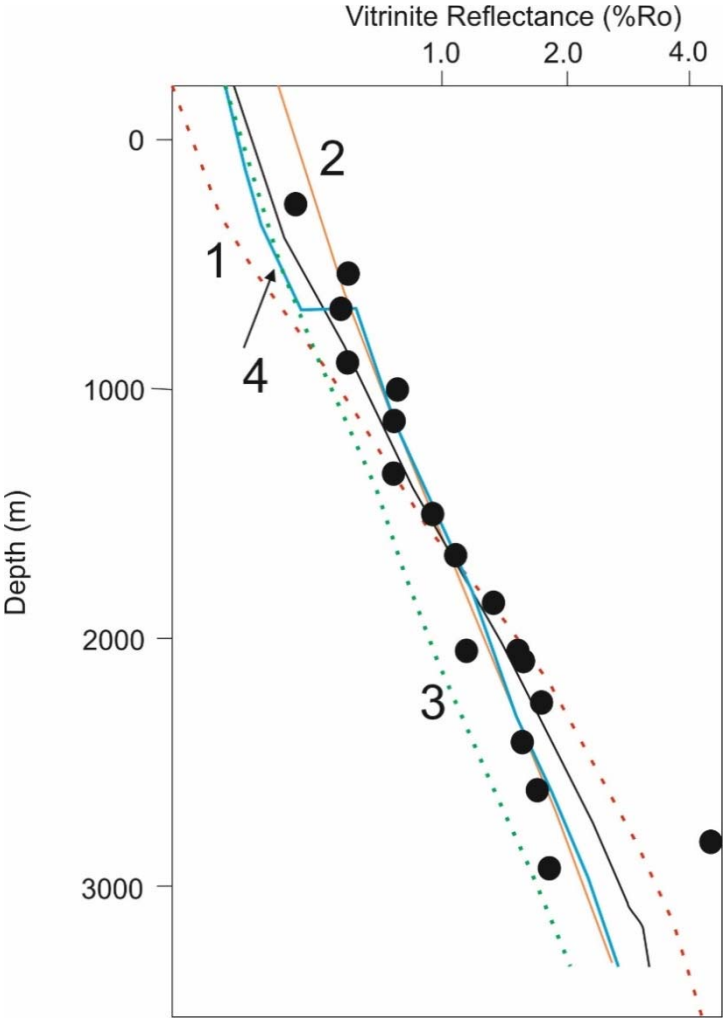

Fig. 17. Graphs of VRr versus depth showing the results of sensitivity analyses. Black line shows the calibration curve for the scenario described in the Results (base case); Scenario 1 (red line) assumes an elevated heat flow of 120 mW/m² during the late Miocene and no Miocene erosion, Scenario 2 (orange line) assumes 1800 m of Miocene erosion and a heat flow of 75 mW/m²; Scenario 3 (green dashed line) shows the calculated vitrinite reflectance curve for Miocene erosion of 900 m and a heat flow of 75 mW/m²; and scenario 4 (blue line) shows Eocene erosion 2000 m and Miocene erosion of 900 m, coupled with a heat flow of 70 mW/m² since the Miocene, and 95 mW/m² during the Eocene.